UNIVERSIDADE FEDERAL DO CEARÁ
CENTRO DE CIÊNCIAS
DEPARTAMENTO DE BIOQUÍMICA E BIOLOGIA MOLECULAR
PROGRAMA DE PÓS-GRADUAÇÃO EM BIOQUÍMICA

FELIPE DE CASTRO TEIXEIRA

INDUTOR APOPTÓTICO DE CONDENSAÇÃO DA CROMATINA NO NÚCLEO: ANÁLISE DE GENOMA EM PLANTAS E PERFIL DE EXPRESSÃO DURANTE O ESTRESSE BIÓTICO EM *vigna unguiculata* [l.] Walp

FORTALEZA
2022

FELIPE DE CASTRO TEIXEIRA

INDUTOR APOPTÓTICO DE CONDENSAÇÃO DA CROMATINA NO NÚCLEO: ANÁLISE DE GENOMA EM PLANTAS E PERFIL DE EXPRESSÃO DURANTE O ESTRESSE BIÓTICO EM *vigna unguiculata* [l.] Walp

Dissertação apresentada ao Programa de Pós-Graduação em Bioquímica da Universidade Federal do Ceará, como requisito parcial à obtenção do título de mestre em Bioquímica. Área de concentração: Bioquímica vegetal

Orientador: Prof. Dr. Murilo Siqueira Alves

FORTALEZA

2022

Dados Internacionais de Catalogação na
PublicaçãoUniversidade Federal
do Ceará
Sistema de Bibliotecas
Gerada automaticamente pelo módulo Catalog, mediante os dados fornecidos
pelo(a) autor(a)

T266i Teixeira, Felipe de Castro.
Indutor apoptótico de condensação da cromatina no núcleo: análise de genoma em plantas e perfil de expressão durante o estresse biótico em Vigna unguiculata [L.] Walp / Felipe de Castro Teixeira. – 2023.
66 f. : il. color.

Dissertação (mestrado) – Universidade Federal do Ceará, Centro de Ciências, Programa de Pós-Graduaçãoem Bioquímica, Fortaleza, 2023.
Orientação: Prof. Dr. Murilo Siqueira Alves.

1. ACIN1. 2. Análise genômica. 3. Morte celular programada. 4. Modulação da cromatina. 5. Filogenia.
I. Título.

CDD 572

FELIPE DE CASTRO TEIXEIRA

INDUTOR APOPTÓTICO DE CONDENSAÇÃO DA CROMATINA NO NÚCLEO: ANÁLISE DE GENOMA EM PLANTAS E PERFIL DE EXPRESSÃO DURANTE O ESTRESSE BIÓTICO EM *vigna unguiculata* [l.] Walp

Dissertação apresentada ao Programa de Pós-Graduação em Bioquímica da Universidade Federal do Ceará, como requisito parcial à obtenção do título de mestre em Bioquímica. Área de concentração: Bioquímica vegetal.

Aprovada em: 25 de fevereiro de 2022

BANCA EXAMINADORA

_____
Prof. Dr. Murilo Siqueira Alves (Orientador)
Universidade Federal do Ceará (UFC)

_____
Prof. Dr. Luciano Fietto
Universidade Federal de Viçosa (UFV)

_____
Dra. Ana Luiza Paiva
Universidade Federal do Ceará (UFC)

A Deus.

E A minha mãe, por todo apoio.

AGRADECIMENTOS

A Deus, pelo dom da vida.

A minha mãe, que sempre me apoiou e sempre me fez levantar a cabeça frente a todos os desafios.

A Nayane Almeida, minha namorada, pela incrível paciência comigo nesse período e por me motivar durante todo o percurso. Dando até carão quando necessário.

Ao Prof. Dr. Murilo Siqueira Alves, pela excepcional orientação, paciência, cuidado e otimismo. Você foi peça fundamental para estimular a minha formação e sou bastante grato por isso. Te vejo no doutorado!

Aos membros do Laboratório de Proteínas Vegetais de Defesa, professor Tadeu, Pedro e Nadine que, em um período tão difícil na ciência brasileira, sempre se mostraram presentes no ambiente de trabalho, dando suas contribuições e estimulando cada um a persistir na pesquisa independente das dificuldades.

A minha memorável amiga de bancada e de mestrado, Erica Monik. Que compartilhou comigo todos os momentos de loucura que foi essa pós-graduação, assim como as nossas demais amigas Josy e Fernanda. Todas sempre prestativas e importantes nessa jornada, tornando o mestrado mais descontraído.

A Sâmia Alves, minha IC, extremamente organizada, sempre ávida por aprender e a participar dos experimentos. Você foi bastante importante tanto nos trabalhos de bancada como nos trabalhos *in sílico*. Junto com os demais membros do laboratório, Patrícia Pontes, Letícia Sales, Ana Carolina, Alex, Axel e Victor, agradeço a todos pela contribuição, pelas risadas e várias conversas no almoço ou nos intervalos do café.

Aos membros do Laboratório de Análise de Sementes (LAS) pelo fornecimento das sementes que foram utilizadas para os estudos deste trabalho.

Aos laboratórios dos professores Thalles, André, Deysi, Hélio, Daniele, Albenísio, Chico e Ana de Fátima, assim todos seus alunos e servidores presentes, que durante todos os experimentos sempre contribuíram com o espaço ou mesmo com a utilização de reagentes, tornando possível a conclusão desse trabalho.

Aos participantes da banca examinadora Prof. Luciano Fietto e Dra. Ana Luiza pelo tempo, pelas valiosas colaborações e sugestões.

À Universidade Federal do Ceará e a todos os funcionários e serviços gerais e professores que contribuem para a instituição fazer seu papel da melhor forma possível.

Aos colegas da turma de mestrado, pelas reflexões, críticas e sugestões recebidas.

A todos demais professores e servidores do DBBM.

O presente trabalho foi realizado com apoio da Coordenação de Aperfeiçoamento de Pessoal de Nível Superior - Brasil (CAPES) - Código de Financiamento 001.

“Os únicos limites das nossas realizações de amanhã são as nossas dúvidas e hesitações de hoje.” (Franklin Roosevelt).

RESUMO

O Indutor Apoptótico de Condensação de Cromatina no Núcleo (ACIN1) é uma proteína *scaffold* capaz de interagir com proteínas ligantes de RNA, tais como a Proteína Ligante de RNA com domínio rico em serina 1 (RNPS1) e a Proteína Associada Sin3A 18 (SAP18). ACIN1 foi descrita pela primeira vez como um componente complexo proteico responsável por desencadear a apoptose em células humanas. Nas plantas, a ACIN1 participa do silenciamento do *Locus Flowering C* (FLC), envolvido na vernalização em Arabidopsis, sem relação clara com o MCP da planta. Ao contrário do verificado em humanos, não há estudos relacionados ao ACIN1 ao MCP em plantas, assim como o conhecimento sobre a função do ACIN1 em plantas é escasso. No presente estudo, realizamos a análise da família genética *ACIN1* em plantas, dando especial atenção à família *Fabaceae*, em vista de um estudo recente relatando a expressão diferencial de uma proteína ACIN1 durante estresse biótico. Identificamos 29 ortólogos *ACIN1* de 19 espécies pertencentes a 12 famílias de plantas. Foram investigados as relações filogenéticas, propriedades físico-químicas, estrutura genética, motivos conservados, cis elementos presentes nos promotores, localização cromossômica, regiões de sintenia e rede de interação. Observou-se grande conservação dos domínios da proteína ACIN1 entre as famílias de plantas. Foi verificado o perfil de expressão gênica do ortólogo ACIN1 de *Vigna unguiculata* durante o estresse biótico, onde a expressão diferencial foi detectada tanto em plantas suscetíveis como resistentes. Possíveis sítios de clivagem de metacaspase foram detectados ao longo das sequências de aminoácidos deduzidos das proteínas ACIN1, mostrando a homologia prevista entre as proteínas vegetais e humanas. Este estudo fornece várias perspectivas de características evolutivas, estruturais e funcionais da família de genes *ACIN1* nas plantas, prevendo sua participação no desenvolvimento das plantas e respostas ao estresse.

Palavras-chave: ACIN1; análise genômica; morte celular programada; modulação da cromatina; filogenia; sintenia; expressão diferencial.

ABSTRACT

Apoptotic Inducer of Chromatin Condensation in the Nucleus (ACIN1) is a scaffold protein capable of interacting with RNA-binding proteins, such as RNA-binding Protein with serine-rich domain 1 (RNPS1) and Sin3A Associated Protein 18 (SAP18). ACIN1 was first described as a complex protein component responsible for triggering apoptosis in human cells. In plants, ACIN1 participates in silencing the Flowering C Locus (FLC), involved in vernalization in Arabidopsis, with no clear relationship to the plant MCP. Unlike in humans, there are no studies related ACIN1 to MCP in plants, as well as knowledge about the function of ACIN1 in plants is scarce. In the present study, we performed the analysis of the ACIN1 gene family in plants, paying special attention to the Fabaceae family, in view of a recent study reporting the differential expression of an ACIN1 protein during biotic stress. We identified 29 ACIN1 orthologs from 19 species belonging to 12 plant families. Phylogenetic relationships, physicochemical properties, gene structure, conserved motifs, cis-elements present in promoters, chromosomal localization, synteny regions and interaction network were investigated. Great conservation of ACIN1 protein domains was observed among plant families. The gene expression profile of the ACIN1 ortholog of Vigna unguiculata during biotic stress was verified, where differential expression was detected in both susceptible and resistant plants. Possible metacaspase cleavage sites were detected along the deduced amino acid sequences of ACIN1 proteins, showing the predicted homology between plant and human proteins. This study provides several insights into evolutionary, structural and functional features of the ACIN1 gene family in plants, predicting their participation in plant development and stress responses.

Keywords: ACIN1; genome-wide analysis; programmed cell death; chromatin modulation; plant phylogenetics; synteny analysis; differential expression.

SUMÁRIO

1 INTRODUÇÃO

1.1 *Vigna unguiculata*

Comum na alimentação de diversos países da África, Ásia e Américas, o feijão-caupi é uma leguminosa que apresenta composição nutricional de proteínas entre 23 a 25% em média, havendo destaque pelo alto teor de fibras alimentares, vitaminas e minerais, além de baixa quantidade de lipídios (cerca de 2%) (FAO, 2020; FROTA; SOARES; ARÊAS, 2008). *V. unguiculata* pode ser cultivada em solos de ambientes tropicais e subtropicais, podendo ter relativa resistência à escassez hídrica e, alguns genótipos, podem resistir ao estresse salino possibilitando bons rendimentos com baixo custo (BASTOS, 2017).

Segundo a FAO (2020), a produção mundial de feijão-caupi, de 1994 a 2018, teve destaque nos países africanos (cerca de 94,9 % de toda a produção durante o período), seguindo pela Ásia com 3 % da produção mundial. Apesar das Américas terem cerca 1,5 % da produção, no Brasil, esse cultivar causa importantes impactos que vão do nutricional ao social (BASTOS, 2017).

Além de fonte alimentar, o feijão-caupi é uma importante fonte geradora de emprego e renda. O feijão-caupi é a base alimentar das populações rurais e urbanas das regiões Norte, Nordeste e Centro-Oeste do Brasil (BASTOS, 2017). A região Nordeste se destaca com a produção desse cultivar, apesar de o Mato Grosso ser o Estado de maior produção no país. A produção de cultivares de porte ereto/semiereto tornou possível a mecanização do cultivo e a obtenção de bons grãos. Dessa forma, o Mato Grosso se tornou uma das maiores regiões de distribuição do Brasil, abrindo o mercado para exportação para diversos países. Em contrapartida, o Ceará e o Piauí, ambos grandes consumidores do feijão-caupi, têm baixa produtividade (kg/ha) desses cultivares devido ao baixo uso de tecnologias e irregularidades pluviométricas. Outros Estados como Maranhão e Pernambuco também têm baixa produtividade (BASTOS, 2017).

Outros aspectos que influenciam a produtividade dessa cultura são as mudanças nas condições edafoclimáticas e a presença de uma diversidade de patógenos e pragas que estão entre os principais problemas associados à produção de feijão-caupi no Brasil e no mundo. Dentre os principais patógenos que afetam a produção de feijão-caupi, vírus são considerados como as principais ameaças ao 7 cultivo do feijão. Oito espécies de vírus apresentam-se como os principais patógenos virais do feijão-caupi: o Vírus do mosaico do

caupi (CPMV, Comovirus)(FA*N et a*l., 2011);Vírus do mosaico severo do caupi (CPSMV, Comovirus) (ABRE*U et a*l., 2012); Vírus do mosaico do caupi transmitido pelo pulgão (CABMV, Potyvirus) (BARRO*S et a*l., 2011); Vírus do mosaico dourado do caupi (CGMV, Begomovirus) (JO*HN et* al., 2008); Vírus do mosaico do pepino (CMV, Cucumovirus) (HU et al., 2012); Vírus do mosqueado clorótico do caupi (CCMV, Bromovirus) (ALI; ROOSSINCK, 2008); e Vírus do mosqueado do caupi (CPMMV, Carmovirus) (BRIT*O et* al., 2012). Dentre todos os vírus citados, o de maior ocorrência no Brasil é o CPSMV (SOUZ*A et* al., 2017).

1.2 Respostas moleculares a estresses bióticos

O mecanismo de defesa das plantas é dividido em duas fases: a resistência basal e resistência induzida (BARI; JONES, 2009). A primeira linha de defesa corresponde à resistência basal que reconhece padrões como: Padrões Moleculares Associados a Patógenos (do inglês, PAMPs), Padrões Moleculares Associados a Dano (do inglês, DAMPs) e Padrões Moleculares Associados à Vírus (do inglês, VAMPs). Esses padrões são reconhecidos por proteínas específicas as quais possuem um domínio receptor extracelular que interage com os padrões moleculares do patógeno (do inglês, PRR) (SOOSAAR; BURCH-SMITH; DINESH-KUMAR, 2005).

As PRRs são proteínas transmembranares que possuem seus domínios na região citoplasmática os quais interagem com uma proteína cinase. Essa interação possibilita a sinalização de possíveis respostas de defesa da célula (SOOSAAR; BURCH-SMITH; DINESH-KUMAR, 2005). A partir da interação com o patógeno pela PRR, alguns eventos são desencadeados a fim de coibir a infecção; dentre eles a sinalização induzida por íons de Ca^{2+} e estresse oxidativo mediado por Espécies Reativas de Oxigênio (ROS), além da indução de expressão de genes relacionados a patogêneses (SOUZA; CARVALHO, 2019).

Essas respostas sistemáticas aos efetores moleculares dos patógenos podem resultar da hipersensibilização (HR) da planta e a morte celular programada (MCP),ocorrendo a indução de expressão de genes de Resistencia Sistêmica Adquirida (do inglês, SAR) (SOUZA; CARVALHO, 2019). A expressão de tais genes é fundamental para a resposta imune da planta pois através deste processo células, tecidos e órgãos vegetais poderão desenvolver resistência à infecção, aumentar o arsenal de defesa contra outros tipos de patógenos, aumentar o tempo de proteção contra estresses bióticos e expressar proteínas que relatam a presença de patógenos no organismo (PR) (SOUZA; CARVALHO, 2019).

Estímulos ambientais também são responsáveis em causar estresses abióticos e bióticos, causando a respostas moleculares. Essas respostas são sinalizadas de forma coordenada por diversos fitohormônios (BARI; JONES, 2009). Fitohormônio como o AS, pode desencadear uma defesa local e o SAR, permitindo uma maior duração na defesa do vegetal. Dessa forma, causando a HR e a não disponibilização de nutrientes para os patógenos que necessitam dos tecidos do hospedeiro vivo para se nutrirem (biotrófico) (GLAZEBROOK, 2005). Outros fitohormônios como Jasmonato (JA) e Etileno (ET), atuam a favor da resistência da planta a patógenos que matam as células para a obtenção dos nutrientes (necrotrófico) (ROBERT-SEILANIANTZ; GRANT; JONES, 2011).

1.3 Morte celular programada em plantas

A MCP é um processo natural e fundamental para a manutenção da homeostase nos seres vivos, envolvendo uma série de fatores para a sua ocorrência e regulação (ZHIVOTOVSKY; ORRENIUS, 2010). Em plantas, a MCP tem suas particularidades quando comparado à MCP em animais, como a presença da parede celular e a ausência de fagócitos que promovem a morte celular ao final do processo (DANON et al., 2000; VAN DOORN, 2011). Apesar dessa diferença, uma das 3 formas de MCP presentes em plantas têm características similares ao dos metazoários, como a retração celular, fragmentação do DNA cromossômico, liberação de citocromo c das mitocôndrias e ativação de proteases(RYERSON; HEATH, 1996; XU; ZHANG, 2009). Outras formas de MCP em plantas envolvem a senescência e a morte mediada por vacúolos. Na senescência, ocorre a degradação do cloroplasto, clivagem de DNA, decomposição da membrana e do vacúolo, além do aumento do nível de fitohormônios como ácido abiscísico (ABA), ET, JA e AS. Por outro lado, a morte mediada por vacúolo tem como característica a ativação de enzimas de processamento vacuolar, assim como a ampliação do vacúolo e o colapso de sua membrana, liberando enzimas de lise e aumentando a acidez da célula (VALANDRO et al., 2020).

Entre essas formas de MCP em plantas, a similar ao mecanismo de defesa dos animais e o de morte mediada por vacúolo, possuem uma Resposta Hipersensível (RH) que causam a condensação da cromatina, fragmentação do DNA, modificações na parede celular, alterações no fluxo de íons e formação de Espécies Reativas de Oxigênio (EROs)(BIRCH et al., 2020; GRANT et al., 2000). Em trabalhos de duplo híbrido com uma espécie mutante de *Arabidopsis thaliana lsd1* cujo genótipo tem respostas mais severas da MCP (JABS;

DIETRICH; DANGL, 1996), a RH mostrou possuir diversos reguladores que a relacionam com metacaspases, dentre outras proteínas associadas a genes como MYB, bZIP, NF-Y, AUX/IAA, LSD1 e PLAC8 (COLL et al., 2010).

A caracterização funcional dos possíveis homólogos de caspases em plantas, as metacaspases (MC), em *A. thaliana*, mostrou que essas proteínas podem clivar sequências ricas em arginina/lisina (RK), e ativarem o processo de apoptose e morte celular em leveduras (WATANABE; LAM, 2005). COLL e colaboradores (2010) verificaram que algumas MC de *A. thaliana* atuavam regulando positivamente a MCP, necessitando de resíduos RK. Diferente dos estudos em humanos, não há estudos envolvendo ACIN1 com a MCP em plantas. Ademais, poucas citações dessa proteína são encontradas no reino vegetal, sendo uma delas realizada por QÜESTA e colaboradores (2016) que estudaram a participação de ACIN1 no processo de silenciamento do gene responsável pelo florescimento em *A. thaliana* durante a ativação da vernalização, não havendo outra relação dessa proteína com o MCP em plantas.

1.4 O Indutor Apoptótico de Condensação da Cromatina 1 (ACIN1)

O Indutor Apoptótico de Condensação da Cromatina 1 (ACINUS ou ACIN1) é uma proteína tipicamente encontrada em animais, havendo diversos trabalhos relatando seu papel funcional em humanos (DEKA; SINGH, 2019; MICHELL*E et* al., 2012). ACIN1 foi descrito pela primeira vez por SAHARA e colaboradores (1999), como o indutor responsável por desencadear o evento de apoptose após sua clivagem pela enzima Caspase-3 além de causar a condensação da cromatina.

ACIN1 apresenta 3 isoformas conhecidas em humanos: Acinus-L, Acinus-S e Acinus-S' (220, 98 e 94 KDa, respectivamente), sendo possivelmente obtidas a partir de um processo de splicing alternativo (DEKA; SINGH, 2019). Essas três isoformas compartilham estruturas tridimensionais semelhantes como um motivo de reconhecimento de RNA e a extremidade C-terminal rica em aminoácidos de serina e arginina (SR) repetidas (DEKA; SINGH, 2019; RODO*R et* al., 2016; VUCETI*C et* al., 2008). DEKA e SINGH (2019) relataram que esse domínio SR está envolvido na regulação de splicing alternativo em células *HeLa*. Cada uma das isoformas de ACIN1 é capaz de interagir com proteínas ligantes ao RNA como as que apresentam domínios ricos em serina (RNPS1), e a proteína SAP18 encontrada associada à proteína desacetilase de histonas Sin3-HDAC. Juntas (ACIN1, RNPS1 e SAP18), formam um

complexo trimérico denominado Complexo de Proteínas Associadas a Apoptose e Splicing (ASAP) (SCHWER*K et a*l., 2003).

Além disso, ACIN1 é um dos fatores que interage dinamicamente ao Complexo de Junção de Exons (EJC) (TANG*E et* al., 2005). O EJC tem impactos diversos em processos pós-transcricionais como o splicing, o transporte e a tradução do RNA mensageiro (mRNA). O EJC liga-se com grande afinidade ao mRNA sem especificidade de sequência. A estrutura desse complexo multiproteico é organizada em torno de um núcleo central de quatro proteínas: elF4A3 (fator de iniciação da tradução em eucariotos), MAGOH (homólogo MAGO; uma subunidade de junção de exons), Y14 (ligante de RNA que reconhece o motivo 8A) e MLN51 (Linfonodo metastático 51, também denominado CASC3) (HIR; SAULIÈRE; WANG, 2016). Dentre as proteínas do complexo, a elF4A3, é capaz de interagir com íntrons e pode co-regular, com a ACIN1-like, eventos relacionados ao splicing e a retenção de introns. Essa regulação do ACIN1-like contempla a inclusão de exon em cassete alternativo a partir da ligação da proteína com o próprio exon, além da ligação com o íntron upstream de células *HeLa* (RODO*R et a*l., 2016). Em paralelo, espécies de *D. Melanogaster* que tiveram *knockdown* do gene *ACIN1*, também tiveram problemas em reter introns durante o splicing (HAYASH*I et* al., 2014). Isso mostra a conservação desse tipo de regulação entre espécies distintas, sobretudo da proteína ACIN1 (RODO*R et* al., 2016).

Figura A – ACIN1 no processamento de RNA. No núcleo, enquanto ocorre a transcrição inicial dos DNA pela polimerase 2, o pré-RNA produzido é associado a agrupamentos de proteínas que formam o splicessomo nos íntrons. A **etapa 1** corresponde também a aproximação das proteínas que compões o EJC. Na **etapa 2**, ocorre aproximação da proteína MLN51 que irá estabilizar o EJC, enquanto as SR e proteínas desconhecidas (?) da via se ligam nos éxons próximos ao ASAP. Na **etapa 3**, fatores de importação nuclear como NXT1 e NXF1 direcionam a saída do RNAm para fora do núcleo, enquanto na **etapa 4**. Após a conclusão da tradução do RNA (não mostrado na figura), a importina (IMP13) com a RAN-GTP estornará as proteínas MAGOH e Y-14 para a **etapa 1**, fechando o ciclo.

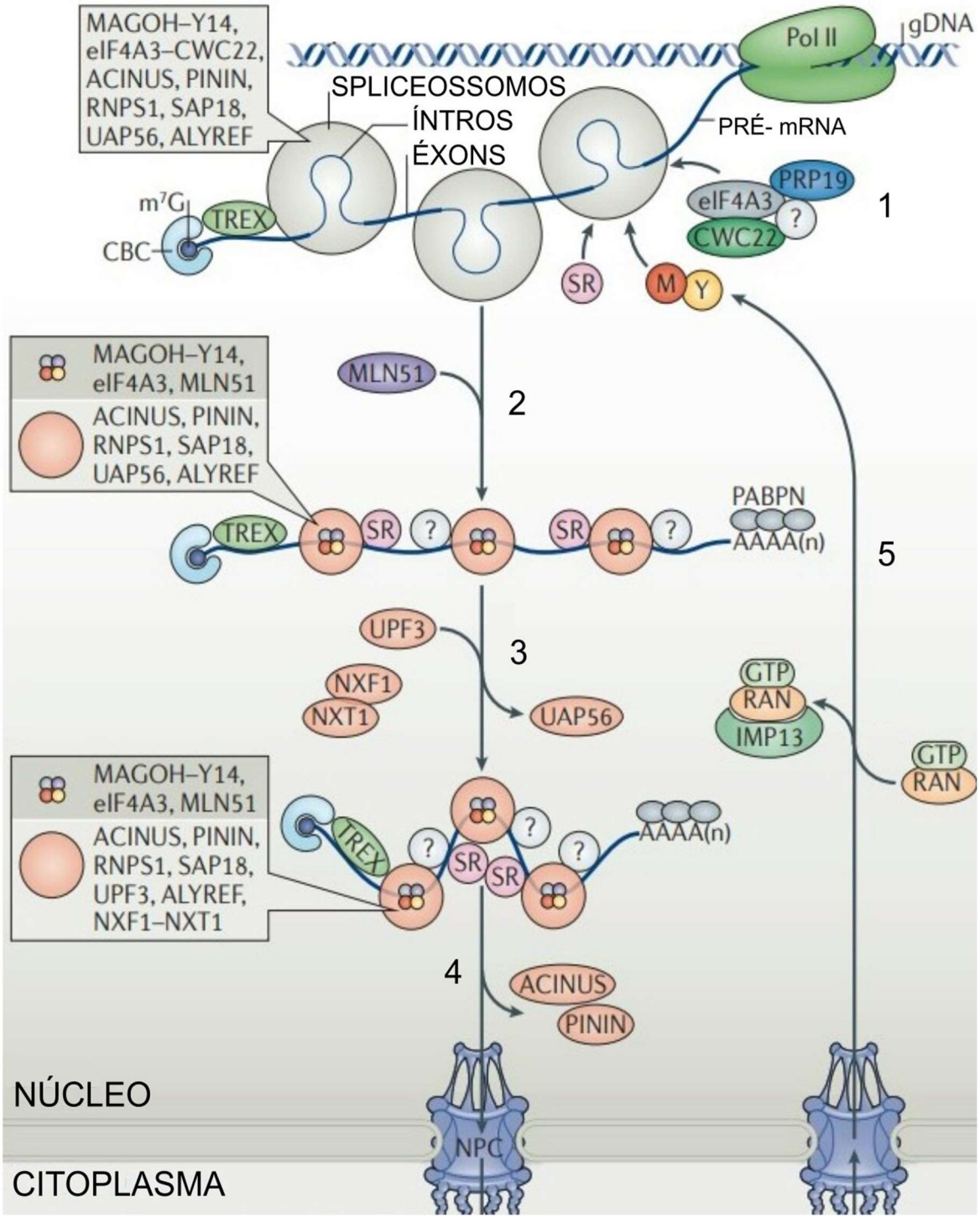

Fonte: (HIR; SAULIÈRE; WANG, 2016)

Em humanos, ACIN1 e a Proteína Associada ao Desmossomo (PININ), formam dois complexos distintos, ASAP (ACINUS, RNPS1 e SAP18) e PSAP (PININ, RNPS1 e SAP18) que têm sua ação de processamento de mRNA no núcleo (MURACHELL*I et a*l., 2012). Essas proteínas deixam EJC pouco antes do mRNA passar pelo Complexo do Poro Nuclear

(NPC), assim como outros fatores presentes no splicessomo tais como o Fator de Exportação Aly/REF (ALYREF). O mecanismo que descreve a remodelagem do EJC após a passagem pelo NPC ainda é desconhecido. No citoplasma, a ausência de atividade de estabilização dos fatores RNPS1 e SAP18 é suprida pelo Regulador de Transcrição nosense (UPF3) (não mostrado na figura A), que pode interagir tanto com RNPS1 como com as proteínas SR (HIR; SAULIÈRE; WANG, 2016)

Esse processamento de mRNA e a ação do EJC e ASAP são bastante conservados entre eucariotos (RODO*R et* al., 2016). Em *A. thaliana*, ACIN1 também está envolvido no processo de silenciamento do gene responsável pelo florescimento da planta durante a ativação da vernalização (QÜEST*A et a*l., 2016). Ademais, estudos de alinhamento de proteínas do ASAP de *A. thaliana* com as que estão presente em animais como *D. melanogaster* e *Homo sapiens*, confirmou que o alinhamento entre esses complexos de proteínas são ortólogas (CHE*N et* al., 2019).

Exceto pela *A. thaliana*, a literatura cientifica não expõe outras funções de ACNI em plantas, apesar de haver sequências homólogas da proteína em espécies vegetais depositadas no *GenBank* e *National Center for Biotechnology Information* (NCBI). Nesse contexto, Paiva e colaboradores (2016) observaram, em *V. unguiculata*, um aumento significativo da expressão de diversos grupos de proteínas seis dias após os cultivares serem inoculados com o vírus do mosaico severo do caupi (CPSMV). A análise proteômica revelou que dentre as proteínas verificadas com significativo aumento de expressão nos cultivares suscetíveis (CE- 31 ou Pitiúba), encontrava-se um ortólogo da proteína ACIN1 (ACIN1-like). Em outro trabalho, uma atividade similar foi realizada por Varela e colaboradores (2017) (VAREL*A et* al., 2017), modificando apenas o cultivar de *V. unguiculata* (Marataoã), resistente à infecção. Seis dias após a inoculação, as folhas não apresentaram sintomas e o perfil proteômico mostrou decréscimo dos níveis de proteínas de defesa no sexto dia, além da ausência da expressão diferencial de ACIN1-like.

Em vista da importância em explorar novas funções de ACIN1, o objetivo desse trabalho consiste em analisar a participação de ACIN1 no desencadeamento da morte celular programada a partir de sua possível clivagem por metacaspase.

2 OBJETIVO

2.1 Objetivo geral

Realizar de genoma da família genética ACIN1 em plantas, bem como avaliar o padrão de expressão do ortólogo de ACIN1 durante o estresse biótico em *Vigna unguiculata*.

3 ARTIGO

***Apoptotic chromatin condensation inducer in the nucleus*: genome-wide analysis in plants and expression profile during Cowpea Severe Mosaic Virus infection in *Vigna unguiculata* [L.] Walp**

Felipe Castro Teixeira[1], Erica Monik Silva Roque[1], Alex Martins Aguiar[1], Sâmia Alves Silva[1], Luciano Gomes Fietto[2], Murilo Siqueira Alves[1*]

[1] Departamento de Bioquímica e Biologia Molecular, Universidade Federal do Ceará, Avenida Humberto Monte S/N, Campus do Pici, Fortaleza, CE, 60440-900, Brazil

[2] Departamento de Bioquímica e Biologia Molecular, Universidade Federal de Viçosa, Avenida PH Rolfs S/N, Campus Viçosa, Viçosa, MG, 36570-900, Brazil

*Corresponding author: murilo.alves@ufc.br

ABSTRACT

Apoptotic Chromatin Condensation Inducer in the Nucleus (ACIN1) is a scaffold protein that was first described as a complex component responsible for triggering apoptosis in human cells. In plants, ACIN1 participates in silencing of *Flowering Locus C* (*FLC*), involved in vernalization in *Arabidopsis thaliana*. Contrary to what has been observed for humans, there are no reports on ACIN1 linking to programmed cell death in plants. Actually, the function of ACIN1 in plants is still poorly understood. In the present study, a genome-wide analysis of the *ACIN1* gene family in plants identified 29 *ACIN1* orthologs from 19 species belonging to 12 plant families. The phylogenetic relationships, physicochemical properties, gene structure, conserved motifs, promoter *cis*-elements, chromosomal localization, syntenic regions, and interaction network were investigated. Altogether, these analyzes revealed highly conserved domains in the structure of the ACIN1 proteins, as well as putative metacaspase cleavage sites, which suggest that they play a conserved function probably associated with the programmed cell death in plants. For instance, differential expression pattern and modulation of *ACIN1* were noticed after inoculation of cowpea with Cowpea severe mosaic virus (CPSMV). Therefore, this study was conducted to provide, for the first time, information on the evolutionary, structural, and functional characteristics of the *ACIN1* gene family as an initial effort towards understanding the role of these proteins in studied plant development and stress responses.

Keyword: ACIN1; genome-wide analysis; programmed cell death; chromatin modulation; plant phylogenetics; synteny analysis; differential expression

4 Introduction

Programmed cell death (PCD) is a fundamental process for homeostasis maintenance in most living beings, involving a plethora of molecular factors for its occurrence and regulation (GREEN, 2019; KERR; WYLLIE; CURRIE, 1972). One of these factors is the Apoptotic Chromatin Condensation Inducer in the Nucleus (ACIN1, or ACINUS). ACIN1 is a well known protein in animals, with studies reporting its functional role in humans (DEKA; SINGH, 2019; MICHELLE et al., 2012; SAHARA et al., 1999). ACIN1 was first described by Sahara and collaborators as one of the proteins responsible for triggering one of the most known apoptosis pathways in *HeLa* cells (SAHARA et al., 1999). ACIN1 is cleaved by Caspase-3, which is related to activate apoptosis-associated chromatin condensation. This pathway is triggered after signaling by the Fas ligand (SAHARA et al., 1999) in the extrinsic apoptosis pathway (CAVALCANTE et al., 2019). Subsequently, Joselin and collaborators suggested ACIN1 may not participate in chromatin condensation, but present a role in genomic DNA cleavage during apoptosis, allowing the activation of apoptotic nucleases and their access to DNA (JOSELIN; SCHULZE-OSTHOFF; SCHWERK, 2006).

After Caspase-3 activation, ACIN1 isoforms can be cleaved, generating a 23 kDa peptide, common to all the isoforms (SAHARA et al., 1999). Besides the studies regarding the participation of ACIN1 during apoptosis, there is a scarcity of information about the function of this protein in other PCD pathways. The three known isoforms of ACIN1 in humans, ACINUS-L, ACINUS-S and ACINUS-S' (202, 98 and 94 KDa, respectively) share similar three-dimensional structures, such as an RNA recognition motif and a C-terminal arginine–serine (RS) rich domain (DEKA; SINGH, 2019; RODOR et al., 2016; VUCETIC et al., 2008). Deka and Singh reported the RS domain is involved in alternative splicing regulation in HeLa cells. Each human ACIN1 isoform is able to interact with RNA-binding proteins, such as RNA Binding Protein With Serine Rich Domain 1 (RNPS1) and Sin3A Associated Protein 18 (SAP18), found associated with the histone deacetylase protein Sin3-HDAC (DEKA; SINGH, 2019).

When compared to PCD in animals, PCD pathways in plants present crucial differences, such as presence and participation of cell wall and absence of phagocytes (DANON et al., 2000; VAN DOORN, 2011). Despite these singularities, some forms of PCD in plants show similar characteristics to PCD in metazoans, such as cell retraction, chromosomal DNA fragmentation, release of cytochrome c from mitochondria and activation of proteases (RYERSON; HEATH, 1996; XU; ZHANG, 2009). Other forms of PCD in plants involve senescence and vacuole-mediated death. In senescence, several cellular and molecular

processes occur, such as chloroplast degradation, DNA cleavage, membrane and vacuole breakdown, and increased levels of senescence-related phytohormones are verified, such as ethylene (ET). On the other hand, vacuole-mediated death is characterized by vacuolar processing enzymes (VPEs) activation, as well as vacuole enlargement and collapse, releasing non-specific lysis enzymes and increasing cytoplasm acidity (VALANDRO et al., 2020). Among all forms of PCD in plants, one of the most similar to that related to cellular immunity PCD in animals is the Hypersensitive Response (HR), which promote chromatin condensation, DNA fragmentation, cell wall modifications, changes in ion flux and generation of Reactive Oxygen Species (ROS) (BIRCH et al., 2020; GRANT et al., 2000).

In a study using *Arabidopsis thaliana lsd1* mutant, whose phenotype present severe PCD responses, HR was modulated by several proteases such as putative caspases homologs in plants, the metacaspases (MC), among other important regulators, such as transcription factor family members like MYB, bZIP and NF-Y, and protein modulators like LSD1 and PLAC8 (COLL et al., 2010). Functional characterization of MC in *A. thaliana* showed these proteins can cleave arginine/lysine-rich (RK) sequences, and activate PCD in yeast (WATANABE; LAM, 2005). COLL and collaborators (2010) found some *A. thaliana* MC acted positively regulating PCD, requiring RS residues (COLL et al., 2010).

Unlike verified in humans, there are no studies relating ACIN1 with PCD in plants. In addition, few studies about ACIN1 function can be found in plants. One of these studies was carried out by Questa and collaborators, showing participation of AtACIN1 in the silencing of *Flowering Locus C* (*FLC*), which is involved in vernalization, with no clear relationship to PCD (QÜESTA et al., 2016). In another recent study, AtACIN1 is *O*-GlcNAcylated and *O*-fucosylated, allowing modulation of transcription and alternative splicing of developmental transitions regulators in *A. thaliana (*BI et al*., 2021)*.

Except for studies in *A. thaliana*, the scientific literature does not expose other functions of ACIN1 in plants, although there are deducted homologous proteins deposited in specialized databases, such as Phytozome (GOODSTEIN et al., 2012), Viggs (SAKAI et al., 2016), NCBI (SAYERS et al., 2022) and TAIR (LAMESCH et al., 2012). However, in a study analyzing infection of susceptible cowpea plants (*Vigna* unguiculata [L.] Walp.) by Cowpea Severe Mosaic Virus (CPSMV), an ACIN1 protein was found to be differentially expressed in 2 and 6 days after inoculation (PAIVA et al., 2016), indicating its possible modulation during plant defense responses against the virus.

From this perspective, in the present work we performed a genome-wide study of *ACIN1* genes present in relevant plant families, focusing specially on members of the *Fabaceae*

family. The phylogenetic reconstruction of *ACIN1* gene family in several plant families was performed, with their gene architecture determined. Regarding the deducted amino acid sequences of plant *ACIN1* orthologs, analysis of physicochemical properties, conserved motifs and domains localization, and putative protease cleavage sites was performed. Among the *Fabaceae* family members, the diploid *V. unguiculata* species was chosen for gene expression analysis, where *VuACIN1* expression was observed in susceptible and resistant plants inoculated with CPSMV, and in plants treated with salycilic acid (SA), along with marker genes expression. Our study represents the first genome-wide characterization of the *ACIN1* gene family in plants, paving the way for structural and functional characterization of orthologs of this gene family in plant species.

5 RESULTS

5.1 Identification and phylogenetic reconstruction of ACIN1 gene family in plants

Seven (7) species from *Fabaceae*, two (2) species from *Poaceae* and one (1) representative from the other plant families deposited in Phytozome version 12 (https://phytozome-next.jgi.doe.gov/) were chosen to verify the presence of *ACIN1* homologs in their genomes. The amino acid sequence of the sole ACIN1 homolog from *A. thaliana* (TAIR accession AT4G39680) was used as a query to BLAST in Phytozome, NCBI (https://www.ncbi.nlm.nih.gov/) and Vigna Genome Server (https://viggs.dna.affrc.go.jp/) databases, totaling 29 coding DNA sequences (CDS) from 19 species belonging to 12 different plant families (Table 1). Among the species are *Vigna unguiculata, Vigna radiata, Vigna angularis, Phaseolus vulgaris, Glycine max, Medicago truncatula,* and *Lotus japonicus*, from *Fabaceae* family; Citrus sinensis, from *Rutaceae* family; *Manihot esculenta*, from *Euphorbiaceae* family; *Gossypium raimondii*, from *Malvaceae* family; *Arabidopsis thaliana*, from *Brassicaceae* family*; Eucalyptus grandis*, from *Myrtaceae* family; *Amaranthus hypochondriacus*, from *Amaranthaceae* family; *Aquilegia coerulea*, from *Ranunculaceae* family; *Ananas comosus*, from *Bromeliaceae* family; *Sorghum bicolor* and *Brachypodium distachyon*, both from *Poaceae* family; *Solanum tuberosum*, from *Solanaceae* family; and *Physcomitrella patens*, from *Funariaceae* family.

Regarding the sequences that were excluded from our further analyses, one (1) ortholog from *A. comosus* (Aco004109) was excluded due to its poor quality, two (2) orthologs were previously identified in *M. truncatula*, but Medtr8g091530 presented no predicted SAP

domain, and *S. tuberosum* contains a putative fourth ortholog (PGSC0003DMG402027531), however, at the time of data collection (March 2021), it presented incomplete sequence.

Table 1 List of plant ACIN1 gene orthologs analyzed in this study, containing plant species, gene ID, chromosomal location, number of ACIN1 orthologs and complete genome size.

Organism	Gene accession	Gene ID	Chromosomal Location	Number of putative ACIN1 orthologs	Genome size (Mb)
Amaranthus hypochondriacus	AH003584	AhACIN1	Scaffold_2:21628495..21632166 forward	1	403.9
Ananas comosus	Aco004109	AcACIN1_1	LG15:1331578..1335865 reverse	2	382
	Aco009582	AcACIN1_2	LG01:1125253..1130253 reverse		
Aquilegia coerulea	Aqcoe6G057500	AcoACIN1	Chr_06:2971605..2976494 reverse	1	306.5
Arabidopsis thaliana	AT4G39680	AtACIN1	Chr4:18414305..18417608 reverse	1	135
Brachypodium distachyon	Brdisv1BdTR5I1002900m.g	BdACIN1_1	pseudomolecule1:11703885..11710984 forward	2	272
	Brdisv1BdTR5I1008689m.g	BdACIN1_2	pseudomolecule_1:37206683..37211189 forward		
Citrus sinensis	orange1.1g004904m.g	CsACIN1	scaffold00487:37826..41369 reverse	1	319
Eucalyptus grandis	Eucgr.I00375	EgACIN1	Chr09:7103963..7109465 reverse	1	641
Glycine max	Glyma.11G237500	GmACIN1_1	Gm11:38068220..38072451 reverse	2	978
	Glyma.18G019700	GmACIN_2	Gm18:1459040..1463695 forward		
Gossypium raimondii	Gorai.N021200	GrACIN1_1	scaffold_371:4081..7502 reverse	3	761.4
	Gorai.003G045500	GrACIN1_2	Chr03:6050870..6055690 forward		
	Gorai.008G102900	GrACIN1_3	Chr08:30938184..30939658 reverse		

Lotus japonicus	Lj6g0021202	LjACIN1_1	chr6:7478465..7483286 forward	2	517.54
	Lj4g0008481	LjACIN1_2	chr4:5657741..5660843 reverse		
Manihot esculenta	Manes.13G090100	MeACIN1_1	Chromosome13:22807939..22816075 reverse	2	639.6
	Manes.13G077700	MeACIN1_2	Chromosome13:21880470..21887591 reverse		
Medicago truncatula	Medtr3g087830	MtACIN1	chr3:39802123..39806174 forward	1	360
Phaseolus vulgaris	Phvul.001G250000	PvACIN1	Chr01:50070922..50074810 reverse	1	537.2
Physcomitrella patens	Pp3c9_18590	PpACIN1_1	Chr09:12576390..12581856 reverse	2	473
	Pp3c15_22110	PpACIN1_2	Chr15:14330566..14335817 reverse		
Solanum tuberosum	PGSC0003DMG402027531	StACIN1_1	ST4.03ch04:62423622..62427432 reverse	3	723
	PGSC0003DMG401027531	StACIN1_2	ST4.03ch04:62433278..62437176 reverse		
	PGSC0003DMG401027531	StACIN1_3	ST4.03ch04:62433278..62437176 reverse		
Sorghum bicolor	Sobic.001G354600	SbACIN1	Chr01:64446914..64451924 forward	1	688.3
Vigna angularis	108329179	VaACIN1	NC_030639.1 (39767685..39771521	1	447.8
Vigna radiata	106756229	VrACIN1	NC_028352.1 (23087517..23091472)	1	459.2

Vigna unguiculata	Vigun01g234400	VuACIN1	Vu01:40608845..40612913 reverse	1	519.4

Phylogeny by Bayesian inference showed posterior probability values equal to 1 in most clades of the consensus tree (Fig. 1), with 0.56 as the lowest posterior probability verified between the cluster of *A. hypochondriacus* and *E. grandis* with the species *A. thaliana*. There was proximity between clusters of *G. raimondii* with *M. esculenta*, with one node representing common ancestry between both representatives of the family. The identification of *PpACIN1* in bryophytes (*P. patens*) suggests the existence of *ACIN1* orthologs in pteridophytes and gymnosperms, as verified in angiosperms (Fig. 1). *P. patens* shares a common ancestor with *B. distachyon*, and this same cluster shares ancestry with the cluster of *S. tuberosum* orthologs. Regarding the number of *ACIN1* genes per species, in *Fabaceae*, except for *V. unguiculata, V. radiata, V. angularis* and *P. vulgaris* (all diploid), all species analyzed presented two *ACIN1* representatives in their genomes. In *M. truncatula*, despite two sequences were obtained using the sequence identification pipeline, just one was represented in our analysis, because the other lacked an SAP protein recognition domain, typically found in *ACIN1* family members. Most plant families presented members in the same cluster, except for two sequences of *B. distachyon,* which differed in gene size, structure (Fig. 2b) and absence of certain protein motifs (Fig. 2c).

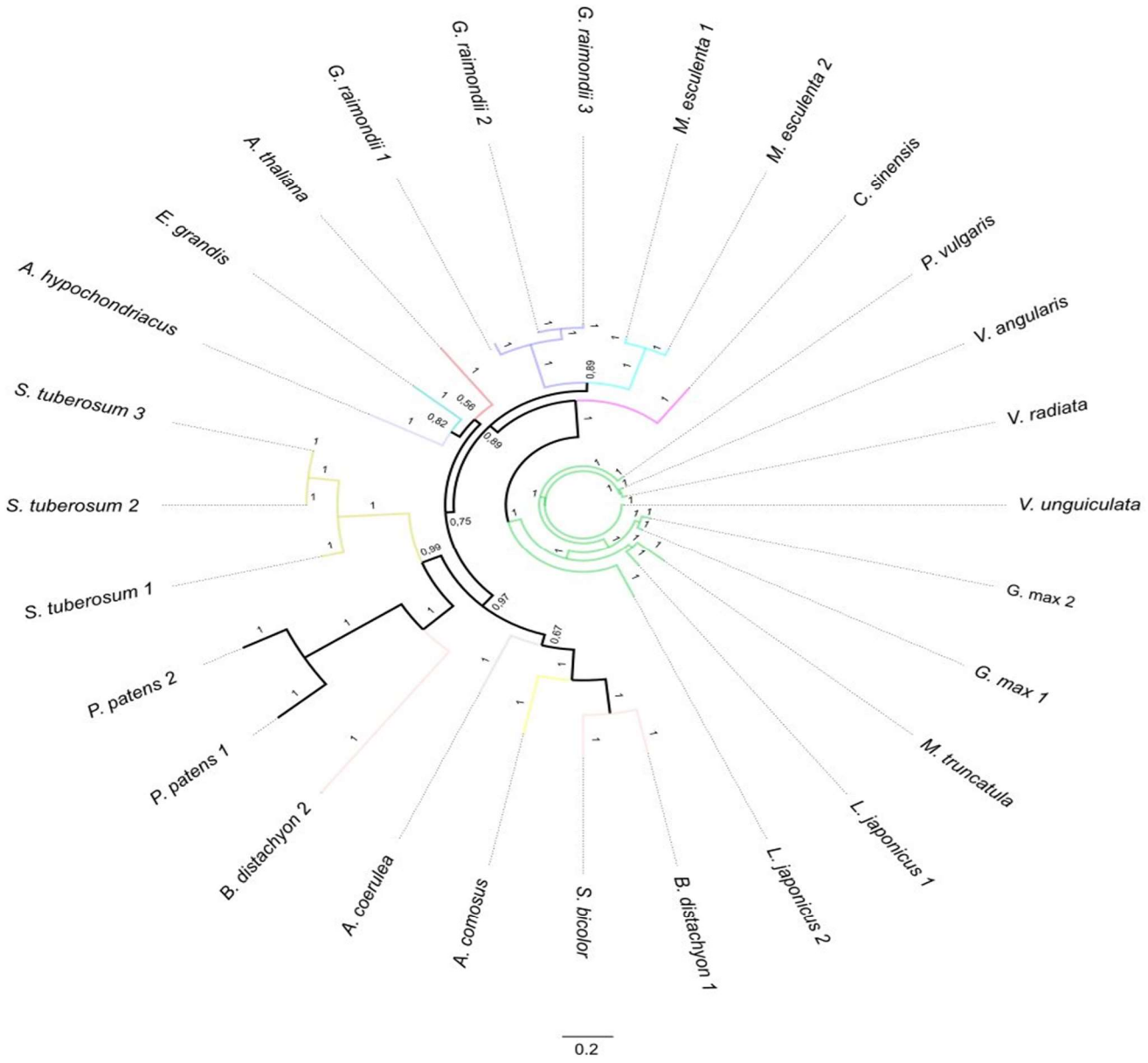
G. raimondii 3
M. esculenta 1
M. esculenta 2
C. sinensis
P. vulgaris
V. angularis
V. radiata
V. unguiculata
G. max 2
G. max 1
M. truncatula
L. japonicus 1
L. japonicus 2
B. distachyon 1
S. bicolor
A. comosus
A. coerulea
B. distachyon 2
P. patens 1
P. patens 2
S. tuberosum 1
S. tuberosum 2
S. tuberosum 3
A. hypochondriacus
E. grandis
A. thaliana
G. raimondii 1
G. raimondii 2
0.2

Fig. 1 Unrooted phylogram of *ACIN1* gene family in plants, by Bayesian inference. Each plant family branch is represented by a specific color: Funariaceae (black), Poaceae (pink), Solanaceae (olive green), Bromeliaceae (lime green), Ranunculaceae (gray), Amaranthaceae (lilac), Myrtaceae (Capri blue), Brassicaceae (red), Malvaceae (blue), Euphorbiaceae (sky blue), Rutaceae (bright pink) and Fabaceae (green). Numbers in taxas and branches correspond to posterior probability. The bar below the phylogram corresponds to the number of nucleotide substitutions

5.2 Physicochemical properties of plant ACIN1 proteins

Using the deducted amino acid sequences of ACIN1 proteins from each plant species, analyses of peptide length, average molecular mass, isoelectric point (IP), average hydrophobicity (GRAVY), and molecule instability were performed (Supplementary Fig. 1). The results showed amino acid sequences ranging from 407 to 874 amino acids (*G. raimondii 3* and *S. tuberosum 1*, respectively). In *Fabaceae*, there was less variation in peptide length among ACIN1 orthologs (Supplementary Fig. 1). Equivalently, the average molecular mass oscillates between 45,519 and 96,152 KDa among species with discrepant lengths. IP values ranged between 4.50 and 4.90 from *B. distachyon 2* and *G. raimondii* 1, respectively. The value corresponding to the protein hydropathicity ranged between -0.945 and -0.622 from *V. radiata* and *P. patens*, respectively, indicating all plant ACIN1 proteins are hydrophilic, corroborating with data verified in humans.

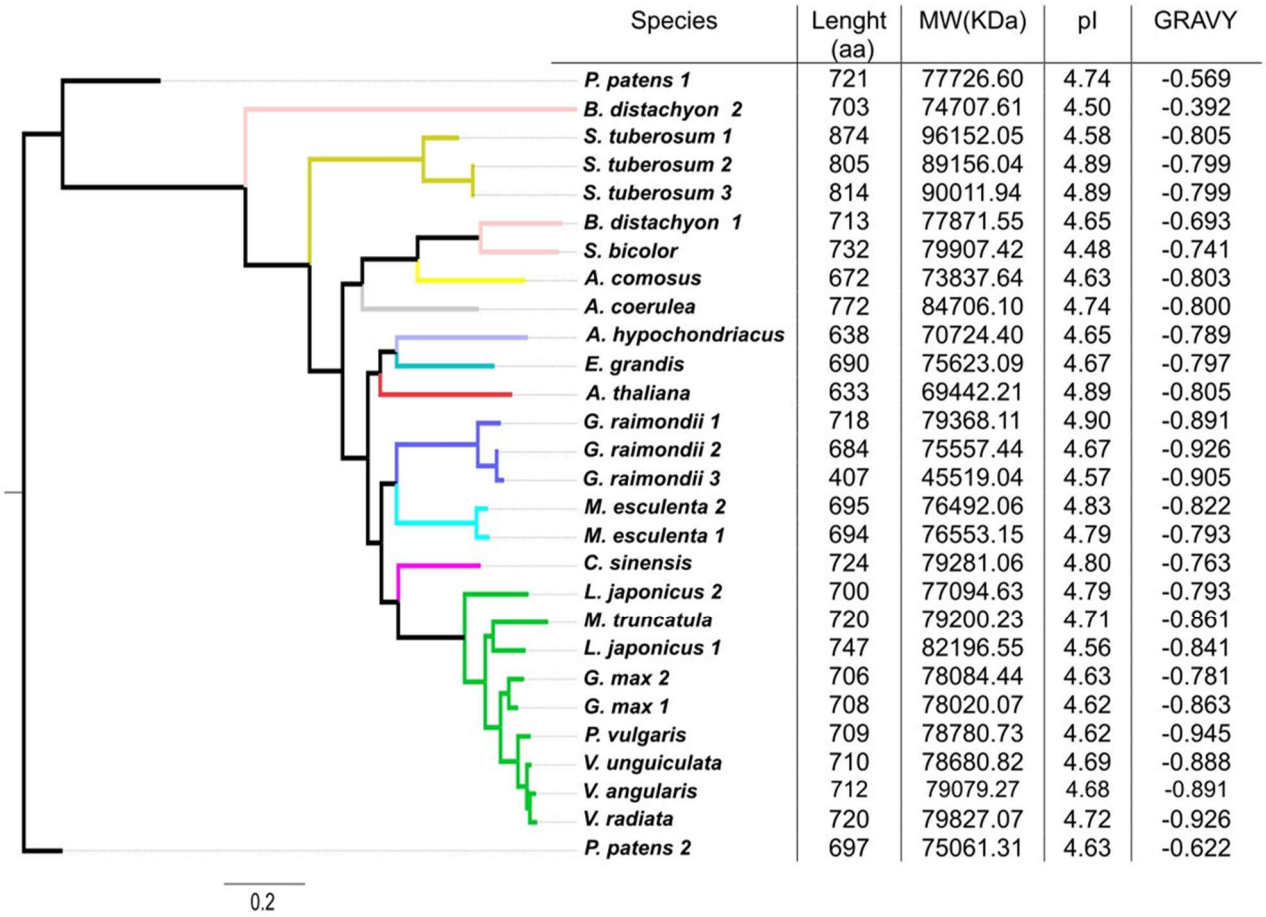

Species	Lenght (aa)	MW(KDa)	pI	GRAVY
P. patens 1	721	77726.60	4.74	-0.569
B. distachyon 2	703	74707.61	4.50	-0.392
S. tuberosum 1	874	96152.05	4.58	-0.805
S. tuberosum 2	805	89156.04	4.89	-0.799
S. tuberosum 3	814	90011.94	4.89	-0.799
B. distachyon 1	713	77871.55	4.65	-0.693
S. bicolor	732	79907.42	4.48	-0.741
A. comosus	672	73837.64	4.63	-0.803
A. coerulea	772	84706.10	4.74	-0.800
A. hypochondriacus	638	70724.40	4.65	-0.789
E. grandis	690	75623.09	4.67	-0.797
A. thaliana	633	69442.21	4.89	-0.805
G. raimondii 1	718	79368.11	4.90	-0.891
G. raimondii 2	684	75557.44	4.67	-0.926
G. raimondii 3	407	45519.04	4.57	-0.905
M. esculenta 2	695	76492.06	4.83	-0.822
M. esculenta 1	694	76553.15	4.79	-0.793
C. sinensis	724	79281.06	4.80	-0.763
L. japonicus 2	700	77094.63	4.79	-0.793
M. truncatula	720	79200.23	4.71	-0.861
L. japonicus 1	747	82196.55	4.56	-0.841
G. max 2	706	78084.44	4.63	-0.781
G. max 1	708	78020.07	4.62	-0.863
P. vulgaris	709	78780.73	4.62	-0.945
V. unguiculata	710	78680.82	4.69	-0.888
V. angularis	712	79079.27	4.68	-0.891
V. radiata	720	79827.07	4.72	-0.926
P. patens 2	697	75061.31	4.63	-0.622

Supplementary Fig. 1 Physicochemical properties of plant ACIN1 proteins. Phylogeny by Bayesian inference, using *P. patens 2* as root. The bar below the phylogram corresponds to the number of nucleotide substitutions. Each ACIN1 ortholog is aligned with the table containing identification and physicochemical properties: molecular mass, pI and GRAVY

5.3 Gene architecture, conserved motif and domain organization in plant ACIN1 gene family

Nucleotide sequences of *ACIN1* genes and deducted amino acid sequences of ACIN1 proteins were used to obtain gene architecture, conserved motif and domain organization, respectively. In *L. japonicus 2*, and in *S. tuberosum* 1, 2 and 3, the 5' and 3' UTR regions were not recognized by GSDS tool (HU et al., 2015). In the other plant species, the arrangement between exons and introns were quite similar, with about 4 or 5 exons detected in most species, reaching 7 in *S. tuberosum 2*; while the number of introns oscillated in most species in around 3 and 4 (Fig. 2b). Gene structure was highly similar among *Fabaceae* members, with exception of *V. radiata*, along with the high similarity verified among *Poaceae*

members, represented by orthologs of *B. distachyon* and *S. bicolor* species. The gene structure showed conservation in the distribution of introns and exons within *Fabaceae* cluster, except for *V. radiata*, which did not present its introns regions recognized by GSDS tool.

Regarding the protein motif analyses, 4 motifs were found, represented by distinct colors in Figure 2. The motifs observed showed high e-value and conservation among sequences (Supplementary Fig. 2 and Supplementary Table 1). The results showed high correlation between the position of the motifs and their location in gene segments, with only two orthologs not showing all 4 motifs: *G. raimondiii 3* and *G. max 2*. SAP and RSB domains (Fig. 2d) were present in the amino and carboxy termini, respectively, of all ortholog sequences, except for *G.max 2*, *G. raimondiii 2* and *G. raimondiii 3*, which lacked the RSB domain. Both motifs and domains presented similar distribution in protein structure of all ACIN1 orthologs.

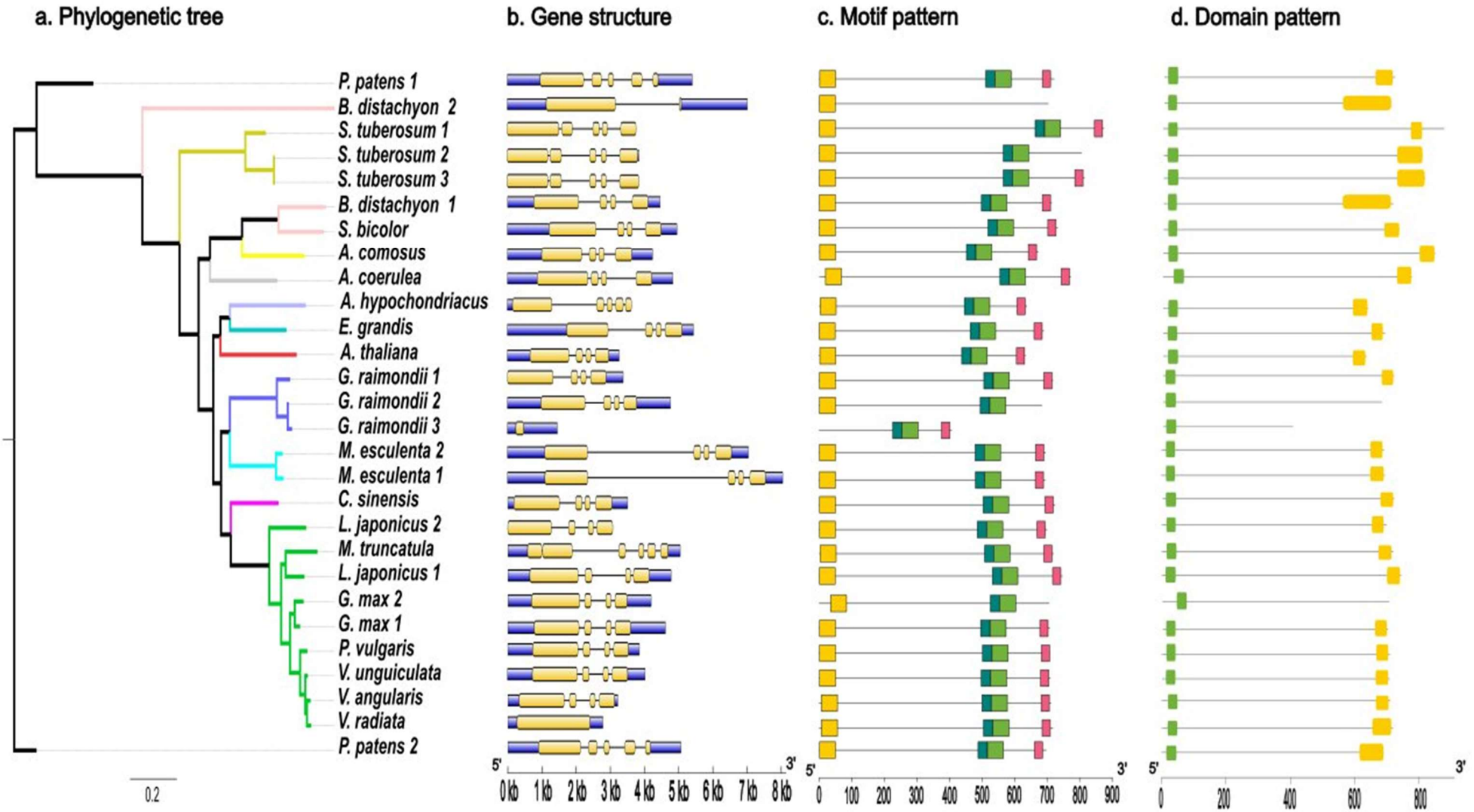
a. Phylogenetic tree
b. Gene structure
c. Motif pattern
d. Domain pattern
P. patens 1
B. distachyon 2
S. tuberosum 1
S. tuberosum 2
S. tuberosum 3
B. distachyon 1
S. bicolor
A. comosus
A. coerulea
A. hypochondriacus
E. grandis
A. thaliana
G. raimondii 1
G. raimondii 2
G. raimondii 3
M. esculenta 2
M. esculenta 1
C. sinensis
L. japonicus 2
M. truncatula
L. japonicus 1
G. max 2
G. max 1
P. vulgaris
V. unguiculata
V. angularis
V. radiata
P. patens 2
0.2
5'
3'
0 kb 1 kb 2 kb 3 kb 4 kb 5 kb 6 kb 7 kb 8 kb
0 100 200 300 400 500 600 700 800 900
0 200 400 600 800

Fig. 2 Evolutionary relationship between taxa, gene structure, conserved motifs and protein domains of *ACIN1* orthologs in various plant species. **a** Phylogram by Bayesian inference. The bar below represents nucleotide substitution. *P. patens* homolog 2 was used as root. **b** Gene structure formed by introns (line), exons (yellow) and 5' and 3' UTR (blue). **c** Conserved motif patterns represented by distinct colors: motif 1 (yellow), motif 2 (blue), motif 3 (green) and motif 4 (pink). **d** Arrangement of SAP (green) and RSB (yellow) domains in ACIN1 proteins. Scales below b, c and d represent number of residues (b, nucleotide; c and d, amino acids)

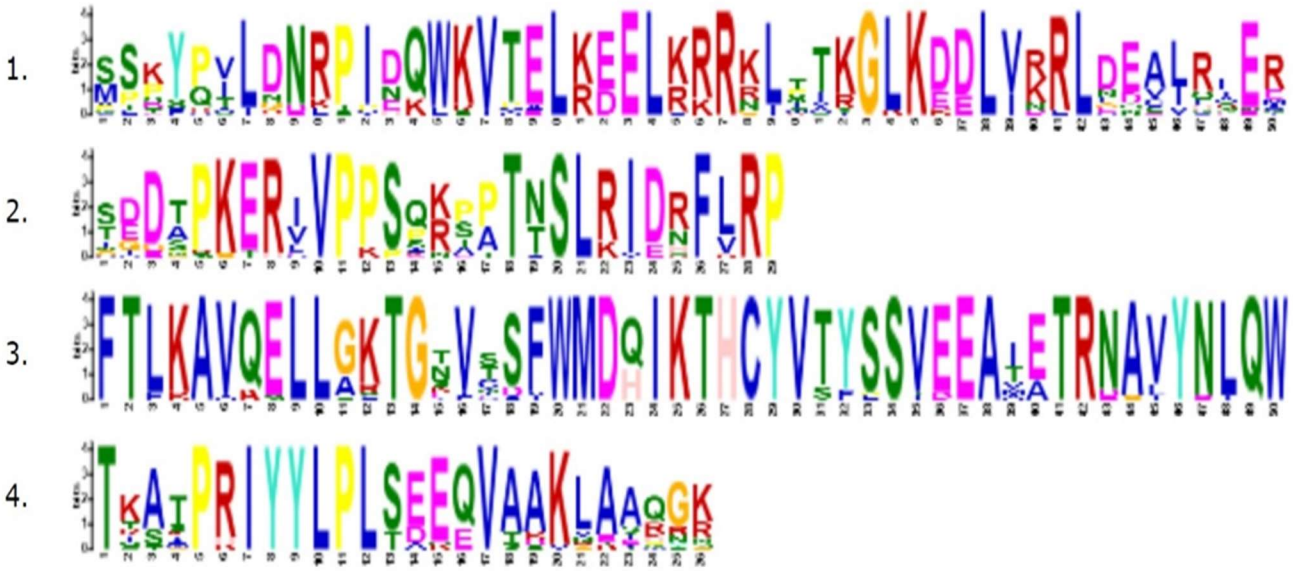

Supplementary Fig. 2 Plant ACIN1 conserved motifs, analysed using MEME. Each number represents a motif in Figure 2c. X axis represents residue position, while Y axis represents information content quality

Supplementary Table 1 List of conserved motifs of ACIN1 proteins in plants

Motifs	Motif consensus	*E*-value
Motif 1 (Yellow)	SSKYPVLDNRPIDQWKVTELKEELKRRKLTTKGLKDDLVRRLDEALRJER	$3.0e^{-800}$
Motif 2 (Dark green)	SDDTPKERIVPPSQKPPTNSLRIDRFLRP	$1.1e^{-452}$
Motif 3 (Light green)	FTLKAVQELLGKTGTVTSFWMDQIKTHCYVTYSSVEEAIETRNAVYNLQW	$1.2e^{-1248}$
Motif 4 (Red)	TKATPRIYYLPLSEEQVAAKLAAQGK	$8.4e^{-371}$

5.4 Putative metacaspase catalytic sites detection

In order to detect putative metacaspase (MC) catalytic sites along the amino acid sequences of ACIN1 proteins, deduced peptide sequences of each ACIN1 ortholog was aligned using ClustalW multiple alignment algorithm (Fig. 3). The results showed the presence of Arginine- and Lysine-rich (RK) sequences in SAP (C-terminal) domain. *V. unguiculata*, *V. radiata*, *V. angularis* and *P. vulgaris*, although not presenting the similarity level verified in other species, still contain RK sequences in their SAP domain. Except for ACIN1 orthologs in *B. distachyon* 2 and the two sequences of *P. patens*, the other peptides contain putative catalytic sites throughout the protein. Specially among *Fabaceae* members, the N-terminal region, where the RSB domain is located, also showed putative catalytic cleavage sites (Fig. 3).

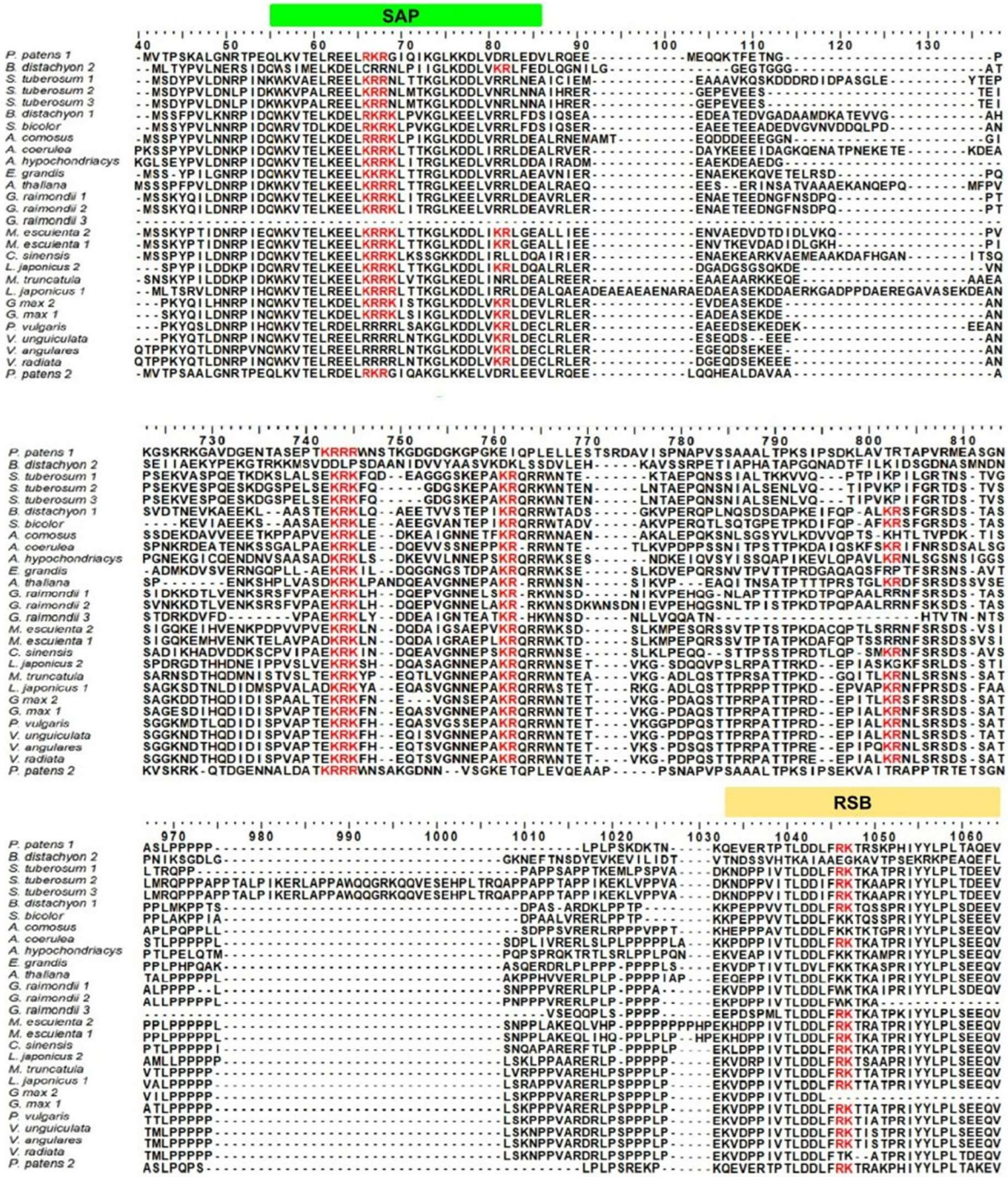

Fig. 3 Putative metacaspase cleavage sites in plant ACIN1 peptide sequences. Above the alignment is represented each residue position. Traces represent gap positions. Segments corresponding to SAP and RSB domains (except for *G. raimondii* 3 and *G. max* 2, which do not present RSB domain) are highlighted by green and yellow boxes, respectively. The red highlighted lysine and arginine (RK) residues show putative metacaspase cleavage sites

5.5 Promoter analysis of plant ACIN1 orthologs

The genomic segment corresponding to 1500 bp of the region upstream the translation start codon of *ACIN1* orthologs was considered for promoter analysis and *cis*-elements prediction (Fig. 4, Supplementary Fig. 3, Supplementary Table 2). Transcription factors can affect the affinity between RNA polymerase and target DNA by binding to specific *cis*-elements present in promoters to regulate transcription of a given gene. We performed promoter analysis of *ACIN1* orthologous genes, and classified the *cis*-elements present according to their main functions, such as responsiveness to hormones, light, stress, growth and development (Fig. 4). *Cis*-elements from uncharacterized groups were classified as undefined. The results showed high prevalence of *cis*-elements associated with responsiveness to growth and developmental stimuli in plants. The *cis*-element ARE was the most abundant among those responsive to stress conditions, such as drought, salinity and extreme temperature, followed by *cis*-elements involved in responses to MeJA (CGTCA), MBS, LTR and P-box. Among the light responsive cis-elements, they were represented by the cis-elements G-box, AE-box, MRE, GATA and I-box. The least abundant group was of hormone responsive motifs, with ABRE (abscisic acid), TGACG, TCA (AS) and AuxRR-core (Fig. 4, Supplementary Fig. 3).

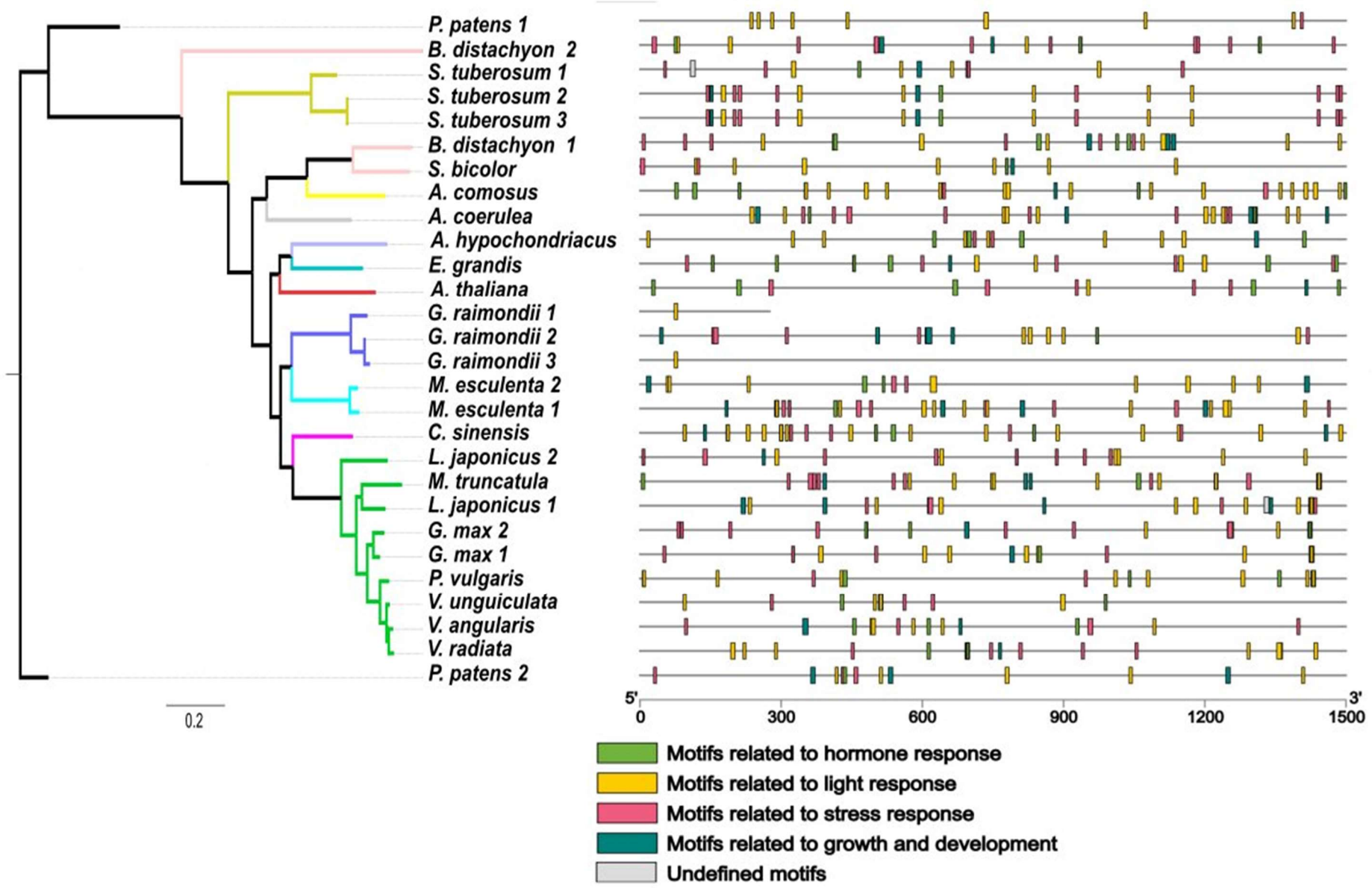
P. patens 1
B. distachyon 2
S. tuberosum 1
S. tuberosum 2
S. tuberosum 3
B. distachyon 1
S. bicolor
A. comosus
A. coerulea
A. hypochondriacus
E. grandis
A. thaliana
G. raimondii 1
G. raimondii 2
G. raimondii 3
M. esculenta 2
M. esculenta 1
C. sinensis
L. japonicus 2
M. truncatula
L. japonicus 1
G. max 2
G. max 1
P. vulgaris
V. unguiculata
V. angularis
V. radiata
P. patens 2
0.2
5'
3'
0
300
600
900
1200
1500
Motifs related to hormone response
Motifs related to light response
Motifs related to stress response
Motifs related to growth and development
Undefined motifs

Fig. 4 Evolutionary relationship between taxa and *cis*-elements of plant *ACIN1* gene members. The promoter region of each *ACIN1* ortholog is represented by lines, where different colored blocks indicate distinct *cis*-elements. Each *cis*-element is classified in specific response groups, as shown below the picture. The scale below the lines represent number of nucleotide residues in the promoter region

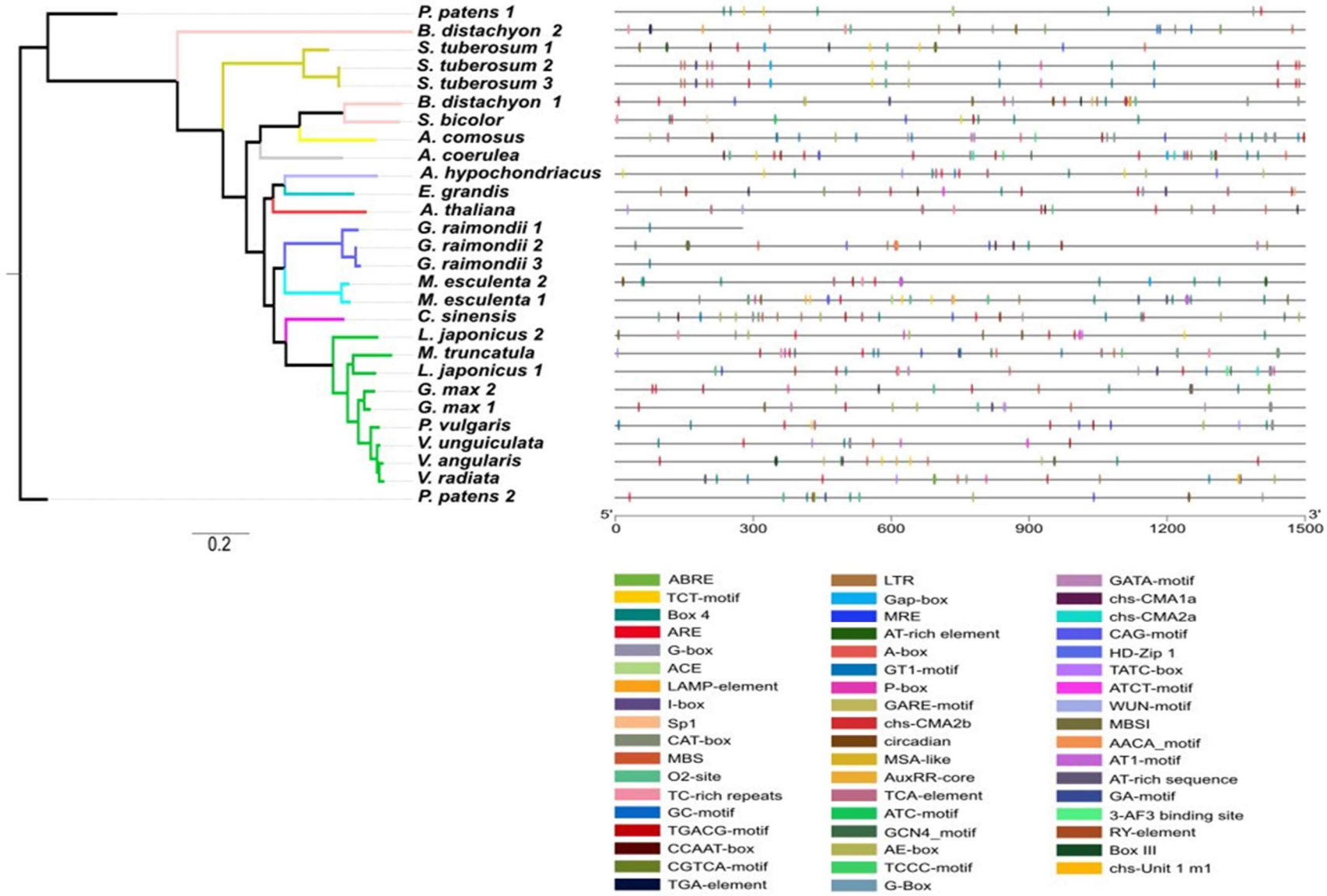
P. patens 1
B. distachyon 2
S. tuberosum 1
S. tuberosum 2
S. tuberosum 3
B. distachyon 1
S. bicolor
A. comosus
A. coerulea
A. hypochondriacus
E. grandis
A. thaliana
G. raimondii 1
G. raimondii 2
G. raimondii 3
M. esculenta 2
M. esculenta 1
C. sinensis
L. japonicus 2
M. truncatula
L. japonicus 1
G. max 2
G. max 1
P. vulgaris
V. unguiculata
V. angularis
V. radiata
P. patens 2
0.2
5'
3'
0
300
600
900
1200
1500
ABRE
TCT-motif
Box 4
ARE
G-box
ACE
LAMP-element
I-box
Sp1
CAT-box
MBS
O2-site
TC-rich repeats
GC-motif
TGACG-motif
CCAAT-box
CGTCA-motif
TGA-element
LTR
Gap-box
MRE
AT-rich element
A-box
GT1-motif
P-box
GARE-motif
chs-CMA2b
circadian
MSA-like
AuxRR-core
TCA-element
ATC-motif
GCN4_motif
AE-box
TCCC-motif
G-Box
GATA-motif
chs-CMA1a
chs-CMA2a
CAG-motif
HD-Zip 1
TATC-box
ATCT-motif
WUN-motif
MBSI
AACA_motif
AT1-motif
AT-rich sequence
GA-motif
3-AF3 binding site
RY-element
Box III
chs-Unit 1 m1

Supplementary Fig. 3 List of all *cis*-elements found in the promoter region of *ACIN1* orthologs in plants. The classification and function of each *cis*-element are shown in Supplementary Table 2

Cis-element	Class	Function	Sequence
ABRE	Hormone responsive	ABA-responsive element	ACGTG
AuxRR-core	Hormone responsive	Involved in auxin response	GGTCCAT
TGACG-motif	Hormone responsive	Involved in the MeJa responsiveness	TGACG
TCA-element	Hormone responsive	Involved in salicylic acid responsiveness	CAGAAAAGGA
TGA-element	Hormone responsive	Auxin responsive	TGACG
GARE-motif	Hormone responsive	Gibberellin responsive	TCTGTTG
TATC-box	Hormone responsive	Cis-acting element involved in gibberellin-responsiveness	TATCCCA
O2-site	Growth and develompment	Cis-acting regulatory element Involved in zein metabolism regulation	GATGATGTGG
Circadian	Growth and develompment	Cis-acting regulatory element involved in circadian control	CAANNNATC
AACA-motif	Growth and develompment	Involved in endosperm-specific negative expression	TAACAAACTCCA
CAT-box	Growth and develompment	Cis-acting regulatory element related to meristem expression	GCCACT
CCAAT-box	Growth and develompment	MYBHv1 binding site	CAACGG
A-box	Growth and develompment	Sequence conserved in alpha-amylase promoters	AATAACAAACTCC
GCN4-motif	Growth and develompment	Cis-regulatory element involved in endosperm expression	TGAGTCA
HD-zip 1	Growth and develompment	Differentiation of the palisade mesophyll cells	CAAT(A/T)ATTG
RY-element	Growth and develompment	Cis-acting regulatory element involved in seed-specific regulation	CATGCATG
MSA-like	Growth and develompment	Cis-acting element involved in cell cycle regulation	TCCAACGGT
Box III	Growth and develompment	Protein binding site	ATCATTTTCA CT
AT-rich element	Growth and develompment	Binding site of AT-rich DNA binding protein (ATBP-1)	ATAGAAATCAA
AT-rich sequence	Growth and develompment	Element for maximal elicitor-mediated activation	TAAAATACT
3-AF3 binding site	*Undefined motif*	Part of a conserved DNA module array	TGAGTCA
LTR	Stress responsive	Cis-acting element involved in low-temperature responsiveness	CCGAAA
ARE	Stress responsive	Cis-acting regulatory element essential for anaerobic induction	AAACCA
GC-motif	Stress responsive	Enhancer-like element involved in anoxic specific inducibility	CCCCCG
P-box	Stress responsive	Gibberellin-responsive element	CCTTTTG
MBS	Stress responsive	MYB binding site involved in drought-inducibility	CAACTG
CGTCA-motif	Stress responsive	Cis-acting regulatory element involved in the MeJA-responsiveness	CGTCA
TC-rich repeats	Stress responsive	Cis-acting element involved in defense and stress responsiveness	GTTTTCTTAC
GA-motif	Stress responsive	Part of a light responsive element	ATAGATAA
WUN-motif	Stress responsive	Stress response element	AAATTACT
MBSI	Stress responsive	MYB binding site involved in flavonoid biosynthetic genes regulation	aaaAaaC(G/C)GTTA
CAG-motif	Light responsive	Part of a light response elemento	GAAAGGCAGAC
TCCC-motif	Light responsive	Part of a light responsive element	TCTCCCT
Sp1	Light responsive	Light responsive element	GGGCGG
GT1-motif	Light responsive	Light responsive element	GGTTAA
G-Box	Light responsive	Cis-acting regulatory element involved in light responsiveness	TACGTG
AT1-motif	Light responsive	Part of a light responsive module	AATTATTTTTTATT
I-box	Light responsive	Part of a light responsive element	GGATAAGGTG
Chs-CMA1a	Light responsive	Part of a light responsive element	TTACTTAA
Chs-CMA2a	Light responsive	Part of a light responsive element	
GATA-motif	Light responsive	Part of a light responsive element	GATAGGA

ACE	Light responsive	Element involved in light responsiveness	GACACGTATG
AE-box	Light responsive	Part of a light responsive element	AGAAACAA
LAMP-element	Light responsive	Part of a light responsive element	CTTTATCA
MRE	Light responsive	MYB binding site involved in light responsiveness	AACCTAA
TCT-motif	Light responsive	Part of a light responsive element	TCTTAC
Gap-box	Light responsive	Part of a light responsive element	CAAATGAA(A/G)A
G-box	Light responsive	Cis-acting regulatory element involved in light responsiveness	TACGTG
ATC-motif	Light responsive	Part of a conserved DNA module involved in light responsiveness	AGTAATCT
Box 4	Light responsive	Part of a conserved DNA module involved in light responsiveness	ATTAAT
Chs-CMA2b	Light responsive	Part of a light responsive element	GAACCTACACAC
Chs-Unit1 m1	Light responsive	Part of a light responsive element	ACCTACCACAC
ATCT-motif	Light responsive	Part of a conserved DNA module involved in light responsiveness	AATCTAATCC

Supplementary Table 2 List of all *cis*-elements found in the promoter region of *ACIN1* orthologs in plants, showing *cis*-element identification, class, function and sequence

5.6 Chromosomal location and synteny of Fabaceae ACIN1 orthologs

Fabaceae members were chosen for further analysis of gene duplication and collinearity. *ACIN1* orthologs presented differences in their positions among species, although they showed a similar distribution along chromosomes (Fig. 5). The collinearity between *V. unguiculata* and other species suggests a putative gene duplication event in *L. japonicus, M. truncatula* and *G. max*, as exposed in the phylogenetic reconstruction (Fig. 1), corroborating with studies highlighting genome duplication in Fabaceae members (CANNON et al., 2006; SCHMUTZ et al., 2010). A double synteny was found between *M. truncatula* and *V. unguiculata,* but only one gene located at chromosome 3 was considered, whose coded protein presents SAP domain in its structure.

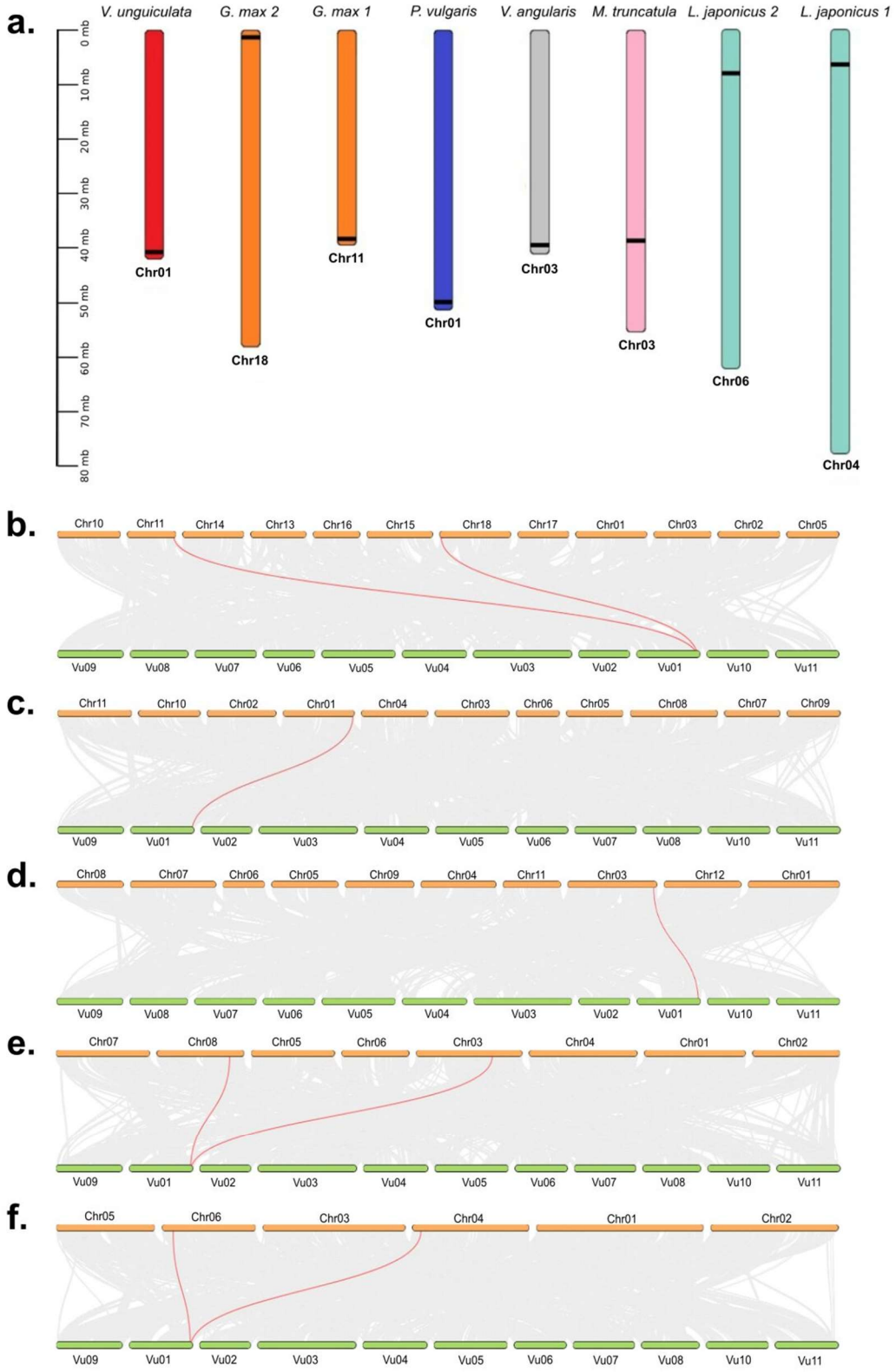

Fig. 5 Chromosomal localization of plant *ACIN1* orthologs in *Fabaceae* species, and their

respective synteny with *V. unguiculata* (*Vu*) chromosomes. **a** Chromosomes from different plant species are represented by distinct colors, with chromosome size and *ACIN1* gene position indicated. **b** Synteny between *G. max* and *V. unguiculata* (*Vu*), **c** *P. vulgaris* and *Vu*, **d** *V. angularis* and *Vu,* **e** *M. truncatula* and *Vu* e **f** *L. japonicus* and *Vu*. *V. unguiculata* chromosomes are represented in green, while chromosomes from other species are indicated in orange. Red lines indicate synteny between *ACIN1* genes, while grey lines indicate global synteny.

5.7 Expression profile V. unguiculata ACIN1 ortholog during CPSMV infection and SA treatment

Considering the large number of diploid members from *Fabaceae* family presenting high phylogenetic proximity and a sole *ACIN1* ortholog (Fig. 1 and Fig. 5), as well as the differential expression of a ACIN1 protein in *V. unguiculata* during biotic stress (PAIVA et al., 2016), the expression profile of *VuACIN1* during CPSMV infection was assessed, as well as during SA treatment (Fig. 6).

VuACIN1 presented a different expression profile between resistant and susceptible *V. unguiculata* plants (Fig. 6a and Fig. 6b), with transcriptional repression at 1 hour after inoculation (hai) in resistant plants and induction at 16 hai in susceptible plants. No significant alteration was detected during SA treatment.

Regarding marker genes expression during CPSMV infection, in resistant plants, *VuMC1* presented repression at 1 hai and induction at 16 hai, while in susceptible plants *VuPR1* presented repression at 1 hai. As a SA marker gene, *VuPR1* was induced at 16 hours after SA treatment (Fig. 6).

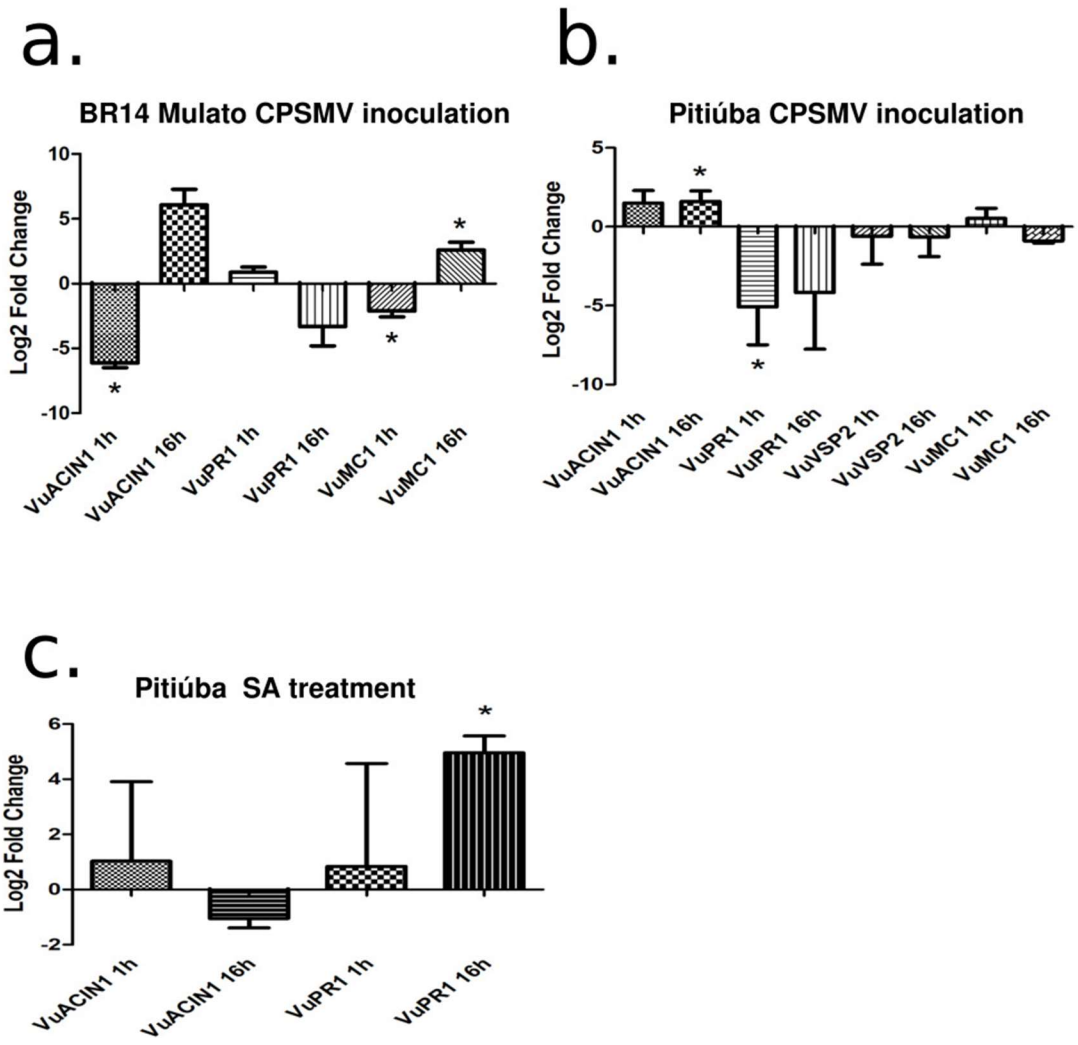

Fig. 6 Expression analysis of *VuACIN1* response to CPSMV in BR14 Mulato (Fig 6.a) and Pitiúba (Fig 6.b). Fig 6.c represent treatment with SA in cowpea leaves. The expression levels were calculated according Pfaffl et al (2001), and statistical significance was obtained according to Yuan et al., (2006) (Pfaffl et al., 2001; Yuan et al., 2006), using nonparametric Mann-Whitney U tests. *VuF-BOX3* and *VuUBQ3* were used as reference genes for CPSMV inoculation and SA application treatments in Pitiúba plants, whereas *VuL23a3* was used as reference gene for CPSMV inoculation treatment in BR 14 Mulato plants. The cDNAs used were obtained from three biological replicates. Means indicated by an asterisk differ significantly from the control treatment at the 5 % significance level. Bars indicate standard error of the means.

5.8 ACIN1 interaction network in Arabidopsis

Using the STRING database (https://string-db.org/), it was verified interaction among AtACIN1, splicing regulators and RNA processing proteins (Fig. 7), characteristics reported by other works, a priori.(RODOR et al., 2016). Proteins such as splicing factor PWI, SAP18, RNA-binding and PABN1, all with co-expression with AtACIN1, suggest the maintenance of functional conservation with regard to RNA processing. Interactions among AtACIN1 and ubiquitin, ubiquitin ligases and histone deacetylases (such as SAP18 and HD1, both with co-expression between them) were verified as well. In this context, SAP18 was considered to have dual actions in both RNA processing and histone deacetylase, knowing that this condition was verified in previous work (SCHWERK et al., 2003). It is interesting to compare that the histone deacetylation actions predicted in *A. thaliana*, when compared in animals, indicate an evolutionary relationship with the characteristic chromatin condensation during apoptosis.

Except for AT5G19340, AT4G31450 and AT4G39690 (uncharacterized protein, U-box and another uncharacterized protein, respectively), all other proteins showed high STRING prediction of interactions: co-occurrence, co-expression, gene fusions, experimentally determined, curated databases, textming, and high values (Scores >0.850). The remaining interactions allowed the formation of the interactome capable of exploring physical and functional information between *A. thaliana* genes.

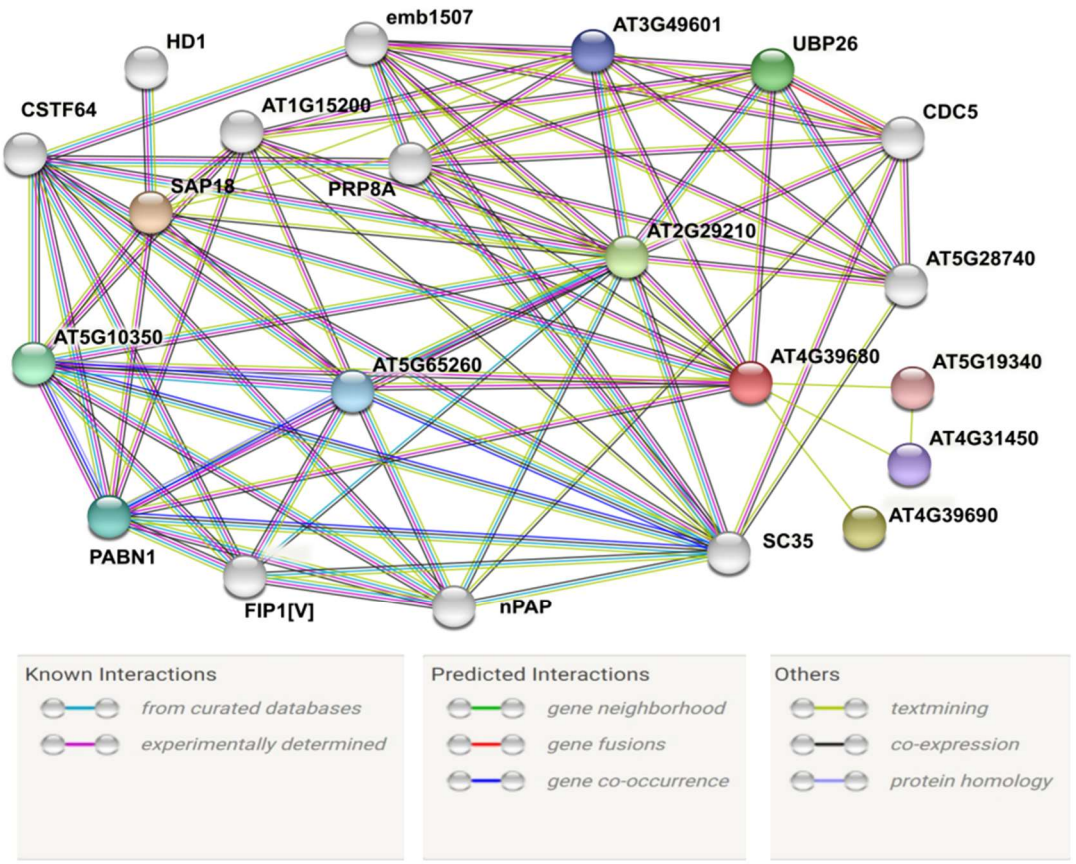

Fig. 7 Interaction network of AtACIN1 protein in *Arabidopsis thaliana*. AtACIN1 is represented by AT4G39680. Circles represent each interacting protein, where colored cycles represent proteins with recognized 3D structure, and uncolored cycles represent proteins with predicted 3D structure. The legend depicts the distinct types of gene interactions verified

6 DISCUSSIONS

With availability of plant genomes in public databases such as Phytozome, genome-wide analysis of whole gene families in several plant species has been made possible using a variety of bioinformatics tools. Such tools have allowed comparative analyses of distinct plant species at molecular level in high resolution. In the present study, orthologous genes of the *Apoptotic chromatin condensation inducer in the nucleous 1* (*ACIN1*) from several plant families were extensively analyzed and compared. Great attention was given to members of *Fabaceae* family, considering the high agronomic relevance of the family (BARKER et al., 1990; HANDBERG; STOUGAARD, 1992; ZHANG et al., 2015). ACIN1 is a scaffold protein that interacts with the proteins SAP18 and RSB, forming a protein complex associated with apoptosis and splicing (ASAP), acting in the context of primary mRNA processing. The joint action of the exon junction complex (EJC) and ASAP in primary mRNA processing is extremely conserved in eukaryotes (RODOR et al., 2016). Among the constituent proteins of ASAP, ACIN1 presents studies relating it to other mechanisms, such as in gene silencing during vernalization in Arabidopsis (QÜESTA et al., 2016). In our study, we included plant gene sequences coding at least the SAP domain, due to its conserved pro-apoptotic action during chromatin condensation and degradation (ARAVIND; KOONIN, 2000).

Despite the large amount of deposited genomic data from several plant species, information about genomic aspects of *ACIN1* gene family in plants is lacking, even with the verified similarities of molecular processes between animals and plants involving ACIN1 members, such as PCD pathways. Some similarities range from cell retraction, DNA cleavage, cytochrome c release from mitochondria, and activation of proteases (RYERSON; HEATH, 1996; XU; ZHANG, 2009). Due to this information gap on *ACIN1* in plants, we performed a genome-wide study of its gene family in several plant species, in which phylogenetic analysis using Bayesian inference (Fig. 1) showed evolutionary linkage among the families analysed. The presence of two *ACIN1* orthologs in some *Fabaceae* members may be related to partial or complete genome duplication, as verified in *G. max (*SCHMUTZ et al., 2010). Genome duplication was also observed in *L. japonicus* by SATO and collaborators (2008) (SATO et al., 2008), in which 315.1 Mb of *L. japonicus* genome presents synteny, corresponding to approximately 91% of all genes. *ACIN1* orthologs remained in their corresponding clusters according to their respective plant family, except for *B. distachyon* 2, that solely formed another branch. This evolutionary distance between two *B. distachyon* sequences is contextualized with results obtained by gene structure and conserved motif distribution analyses (Fig. 2). While

most species maintained conservation of most motifs detected, *B. distachyon* 2 showed absence of 3 motifs in carboxi terminal region. Nevertheless, this sequence maintained conservation of both SAP and RSB domains. Even with RSB domain located in region close to motif 4 position, the absence of this motif showed a possible non-correlation with RSB domain in *B. distachyon* 2. This can also be visualized in *G. raimondiii* 3, which contains motif 4 but lacks RSB domain. Both motif and domain distributions were similar in ACIN1 orthologs, indicating high conservation of this protein between species.

A large clade containing *P. patens* 2 and other species was formed in the phylogram, with several subsequent branches (Fig. 1), indicating strong conservation among *ACIN1* homologs. We can compare this results with data from a study showing protein structure conservation in ASAP complex of *A. thaliana,* whose alignment confirmed orthology with *Drosophila melanogaster* and *H. sapiens* (CHEN et al., 2019).

Unlike the similar features of *ACIN1* genes and proteins in plants, the *cis*-elements present in the promoter region were quite variable. The most predominant class of cis-elements, apart of enhancers and CAAT-box, were light-responsive elements (Fig. 4). Among development and growth-related cis-elements, 87% of them correspond to CAAT-box. Other elements of this class were in a few number compared to other classes. There are traces of circadian motifs, A-box, Box-III and CAT-box, indicating relevance of light regulation for plant *ACIN1* orthologs. Cis-elements responsive to hormones were scarcely found in *Fabaceae* members, with CGTCA (MeJA) and TCA (SA) prominent in other species such as *S. bicolor* and *S. tuberosum*. Despite this, TCA motif was detected in some *Fabaceae* species such as *V. angularis* and *G. max*, suggesting that, during the course of evolution, there was a decrease in presence of hormone regulators in the promoter region of *ACIN1* genes. This was consistent with our qPCR results on *V. unguiculata* treated with SA, where no significant *V. unguiculata ACIN1* ortholog (*VuACIN1*) expression was observed in 1 and 16 hours after treatment, whereas *VuPR1* was overexpressed (Fig 7c). Although no SA-related *cis*-elements was detected in its promoter region, *VuACIN1* presents two cis-elements responsive to MeJA, CGTCA and TGACG, (Fig. 4) suggesting possible participation of *VuACIN1* in defense responses against necrotrophic pathogens, herbivory or wounding (BARI; JONES, 2009). After a wound stimulation, such as carried out during CPSMV inoculation, jasmonate signaling pathway may culminate in *VuACIN1* transcription (Fig 7a and 7b), a hypothesis to be further confirmed.

Regarding stress-responsive *cis*-elements detected in the promoter region of *ACIN1* orthologs, there was a similar pattern in all species analyzed, with an equivalent distribution of ARE (Anaerobic Responsive Element), the most abundant *cis*-element from this group.

Participation in gene silencing during vernalization in *A. thaliana* (QÜESTA et al., 2016) and differential expression in *V. unguiculata* susceptible plants infected with CPSMV (PAIVA et al., 2016) demonstrate the wide range of stimuli that can modulate *ACIN1* action in plant species.

Chromosomal localization and synteny among of different *ACIN1* orthologs in *Fabaceae* family showed similarities among species (Fig. 5). *P. vulgaris* and *V. unguiculata* showed similarities that had been verified in other studies (LONARDI et al., 2019; MUÑOZ-AMATRIAÍN et al., 2017), such as arrangement of the genomic region corresponding to *ACIN1* among species and collinearity among different chromosomes (Fig 6). In synteny between *V. unguiculata* and other species, chromosome 1 of *V. unguiculata* showed double collinearity with other *Fabaceae* members. This result strongly suggests *ACIN1* duplication in *L. japonicus*, *G. max* and *M. truncatula*. Genome duplication in *L. japonicus* and *G. max* has been previously studied (SATO et al., 2008; SCHMUTZ et al., 2010). Furthermore, synteny results of partial genomes of *M. truncatula* and *L. japonicus* suggests their duplications preceded speciation (CANNON et al., 2006). *ACIN1* duplication is maintained in the evolutionary pathway until the emergence of *G. max*, which shares an ancestral node with the subcluster of *P. vulgaris*, *V. unguiculata*, *V. angularis*, and *V. radiata* (Fig 1). Chromosomal localization and synteny between members of these subcluster (Fig 6), on the other hand, may indicate loss of *ACIN1* duplicity after speciation.

Despite differing in size and molecular mass, ACIN1 proteins showed similar low pI as well as negative GRAVY values (Supplementary Fig. 1), indicating ACIN1 proteins are hydrophilic. The pI values less than 5 match the perspective of efficient action at slightly basic pH in the nucleus (KIRAGA et al., 2007), subcelullar compartment where ACIN1 interacts with SAP18 and RNPS1(MURACHELLI et al., 2012).

With exception of action in EJC complex, ACIN1 function in plant cytoplasm is poorly known. From this perspective, putative action of metacaspase (MC) on ACIN1 proteins was evaluated, according to the caspase cleavage sites proposed by Watanabe and Lam (2005). The alignment of ACIN1 proteins indicated presence of conserved RK-rich regions, predominantly in SAP domain, and two other RK-rich regions, one of them in RSB domain (Fig. 3). This result becomes relevant when analyzed in conjunction with the work of Watanabe and Lam (2005), who performed functional characterization of *A. thaliana* MC, noting AtMCP1b and AtMCP2b act by cleaving RK-rich regions and activating programmed cell death (PCD) in yeast. Furthermore, two *A. thaliana* MC acted antagonistically: AtMC1 inducing PCD, requiring RK residues, and AtMC2 repressing PCD, being catalityc residues independent (COLL et al., 2010).

In BR 14 Mulato, a *V. unguiculata* cultivar resistant to CPSMV (SILVA et al., 2012), concomitant repression was observed for V*uACIN1* and *VuMC1* at 1 hour after CPSMV inoculation, while induction of *VuMC1* was observed at 16 hours, but with no significant induction of V*uACIN1* at this time point (Fig. 6a). On the other hand, in Pitiúba, a *V. unguiculata* susceptible cultivar, induction of *VuACIN1* expression occurred at 16 hours, but no significant induction is verified for *VuMC1* (Fig. 6b). Participation of more than one MC protein in plant PCD processes may explain divergence in expression. MC orthologs from *V. unguiculata* may differ in function during PCD compared to AtMCP1b and AtMCP2b from *A. thaliana* (COLL et al., 2010). Another perspective that may explain differences in *VuMC1* expression between cultivars is resistance mechanism to CPSMV in *V. unguiculata*. Significant induction of *VuMC1* expression at 16 h in resistant plants may be result of signaling pathways triggering PCD as part of plant defense against CPSMV infection. Yet, concomitant repression of *VuACIN1* and *VuMC1* at early time points after CPSMV inoculation in resistant plants may indicate VuACIN1 and MC1 joint action being repressed by defense responses, hypothesis to be experimentally confirmed.

Analyzing the expression profile of marker genes, it was observed *VuPR1* had no differential expression in both cultivars when subjected to CPSMV inoculation over time (Fig 7a and Fig7b). This result contrasts with the verified during SA treatment, where *VuPR1* was induced (Fig 7c), being a classic SA marker gene (FU et al., 2012). *VuVSP2*, known as a marker gene for jasmonate response (BERGER et al., 1995), wounding responses (TAKI et al., 2005) and oxidative stress (MIRA; MARTÍNEZ; PEÑARRUBIA, 2002) was poorly expressed in susceptible plants (Fig 7b). Our results in resistant plants indicate plant defense response against CPSMV infection is not SA-dependent. On the other hand, when expression data from susceptible plants are analyzed, we also conclude JA-dependent plant defenses are not modulated during CPSMV infection, indicating other biotic stress responses may be deployed against CPSMV infection. Being obligate parasites, during evolution, viruses have acquired capacity to manipulate host plant cellular machinery. Through viral proteins with multiple functions, the parasitized cell is manipulated while having its defenses reduced (SOUZA; CARVALHO, 2019). Interestingly, in Pitiúba plants, 2 days after CPSMV inoculation, the proteomic profile presents a massive reduction of several protein classes, such as stress/defense, redox homeostasis, plant signaling, protein and RNA/DNA metabolism (PAIVA et al., 2016), indicating direct viral interference in plant translation machinery.

The scaffold feature of ACIN1 proteins impelled us to perform *in silico* interaction analysis in the model species *A. thaliana* (Fig. 7). Except for AT4G39690 (membrane lipid

distribution regulator), AT5G19340 (uncharacterized protein) and AT4G31450 (ubiquitin ligase), the AtACIN1 interaction network presented good overall quality. The well known role of AtACIN1 in RNA processing is contextualized from interactions with proteins such as emb1507 (RNA helicase U5), AT3G49601 (pre-mRNA splicing factor), AT5G10350 (involved with poly(A) grout formation) and AT2G29210 (PWI factor which converts primary mRNA to mature mRNA) (Fig. 7). In parallel, SAP18 and histone deacetylase 1 (HD1) are present in the network, both involved with histone deacetylation process. SAP18 allows interaction between histone deacetylase complex and transcriptional repressors of chromatin (SONG; GALBRAITH, 2006), whereas HD1 performs lysine deacetylase action on N-terminal region of histones (FONG; TIAN; CHEN, 2006). Deacetylase action increases interaction between DNA and histones, promoting chromatin condensation (GALLINARI et al., 2007; SCHWERK et al., 2003), a feature also associated with ACIN1 during apoptosis (SAHARA et al., 1999).

7 CONCLUSIONS

In our study, we highlight three mains aspects regarding the *Apoptotic chromatin condensation inducer in the nucleus* (*ACIN1*) gene family in plants: firstly, a high structural conservation of *ACIN1* orthologs within and among the plant families analyzed, from bryophytes to angiosperms (Fig. 1 and Fig. 2); secondly, the very low number of *ACIN1* orthologs in plant species, where most of the organisms observed present only one *ACIN1* representative (Fig. 1 and Fig. 5); Finally, the high similarity of plant proteins ACIN1 to its human counterpart suggests a role in programmed cell death (PCD) and chromatin condensation. (Fig. 3 and Fig. 7). ACIN1 participation in environmental PCD (ePCD) is suggested, due to its differential expression pattern and modulation during biotic plant stress responses (Fig. 4 and Fig. 6; PAIVA et al., 2016), an important hypothesis to be further confirmed using reverse genetics assays, such as Virus Induced Gene Silencing (VIGS).

The presence of highly conserved putative metacaspase (MC) cleavage sites inside SAP and RSB domains (both also present in the human ACIN1 protein) (Fig 3), as well as the interaction network in *Arabidopsis thaliana* involving SAP18 and histone deacetylase 1 (HD1) (Fig 7), denote function homology between plant and human ACIN1 proteins. Such features instigate further analysis regarding caspase-like activity targeting ACIN1, and ACIN1 involvement in apoptotic-like chromatin condensation in plants, such as *in vitro* enzymatic caspase assays and flow cytometry, respectively.

As the first genome-wide study about *ACIN1* gene family in plants, our results may pave the way for future research about the role of *ACIN1* orthologs during distinct PCD

processes, such as involving pathogen responses or developmental stimuli.

8 Material and methods

8.1 Molecular phylogeny of ACIN1 orthologs in plants

For the phylogenetic reconstruction of plant *ACIN1* gene family, the coding DNA sequences (CDS) of *Vigna unguiculata, Vigna radiata, Vigna angularis, Phaseolus vulgaris, Glycine max, Medicago truncatula, Lotus japonicus, Citrus sinensis, Manihot esculenta, Gossypium raimondii, Arabidopsis thaliana, Eucalyptus grandis, Amaranthus hypochondriacus, Aquilegia coerulea, Ananas comosus, Sorghum bicolor, Brachypodium distachyon, Solanum tuberosum* and *Physcomitrella patens* were collected. The sequences were submitted to MEGA7 software (KUMAR; STECHER; TAMURA, 2016)for multiple alignment using the MUSCLE algorithm. The resulting alignment was manually edited, with gaps above 3 codons removed when present in more than half of the sequences. The resulting alignment was employed to infer the phylogenetic model by Bayesian analysis using MrBayers version 3.2.7, available on CIPRES Science Gateway V3.3 (https://www.phylo.org/), a public server designed for phylogenetic tree inferences, using 10.000.000 generations. FigTree version 1.4.4 was used to phylogram generation.

8.2 Plant ACIN1 orthologs identification

The identification of plant *ACIN1* orthologs was performed in three sequential steps, with use of different searching algorithms for validation, according to similar analyses in recent studies (KUMAR; STECHER; TAMURA, 2016; LI et al., 2021). Firstly, CDS and deducted amino acid sequences of plant *ACIN1* orthologs were obtained from Phytozome database (https://phytozome-next.jgi.doe.gov/) through BLAST, using the AtACIN1 amino acid sequence as query (TAIR access AT4G39680.1). NCBI database (https://www.ncbi.nlm.nih.gov/) was also used, to search *V. radiata* sequences, and Vigna Genome Server database (https://viggs.dna.affrc.go.jp/) was used to search *V. angularis* sequences. Secondly, the deducted peptide sequences obtained from BLAST searches were submitted to domain screening using Hidden Markov Chain (HMM) in Pfam (https://pfam.xfam.org/) and InterPro (https://www.ebi.ac.uk/interpro/) databases, which were validated using the curated UniProt database (https://www.uniprot.org/). Finally, each sequence was double-checked using PSI-BLAST and NCBI-CDD (https://www.ncbi.nlm.nih.gov/Structure/cdd/wrpsb.cgi) at NCBI, which use Position-Specific

Scoring Matrices (PSSMs). Sequences showing *e*-values lower than 10^{-4} in each step presenting the SAF-A/B, Acinus and PIAS (SAP) domain confirmed in all databases were selected for further analyses.

8.3 Analysis of physicochemical properties of plant ACIN1 proteins, and conserved motif and domain search

The physicochemical properties of all deducted ACIN1 proteins were obtained using ProtParam (https://web.expasy.org/protparam/). Conserved ACIN1 motifs were observed using MEME v5.4.1 (https://meme-suite.org/meme/tools/meme). Protein domain data was obtained using Pfam database. Both motif and domain localization data were plotted using TBtools software version 1.098661(CHEN et al., 2020).

8.4 Chromosomal location of plant ACIN1 orthologs

To define the location of *ACIN1* genes on chromosomes, CDS and respective genomic sequences of *ACIN1* genes were collected from Phytozome, NCBI and Vigna Genome Server databases. Chromossome locations were plotted using GSDS software version 2.0.

8.5 Plant ACIN1 promoter analysis

In order to obtain the promoter region of each orthologous gene, a genomic region of 1500 base pairs upstream the translation start codon of the each target gene was used and submitted to PlantCARE tool (http://bioinformatics.psb.ugent.be/webtools/plantcare/html/), aiming the prediction of TATA-box and *cis*-elements described in plants. The TATA-box cis-elements were removed from the analyses, and the remaining *cis*-elements were classified according to responsiveness to phytohormones, light, stress, plant growth and development. *Cis*-element localization data was plotted using TBtools software.

8.6 Synteny analysis

The Dual Systeny Plot for MCScanX tool, embedded in TBtools software, was employed to detect synteny between *V. unguiculata* genome and other *Fabaceae* genomes. *ACIN1* colinearity was displayed using TBtools software.

8.7 Arabidopsis ACIN1 interaction network

AtACIN1 interaction network (TAIR access AT4G39680.1) was retrieved using STRING version 11.5, with cut-off of 0,07 for high confidence interactions.

8.8 Plant materials

Seeds of cowpea (*V. unguiculata* [L.] Walp.), cultivar Pitiúba, susceptible to *Cowpea Severe Mosaic Virus* (CPSMV), and cultivar BR 14 Mulato, resistant to CPSMV, were obtained from the Laboratory of Seed Analysis (LAS) of Universidade Federal do Ceará (UFC). All organisms used in the present work were registered in SISGEN (Sistema Nacional de Gestão do Patrimônio Genético e do Conhecimento Tradicional Associado), under accession A0E5BE1. Seed surfaces were disinfected with 1% (v / v) hypochlorite (0.05% active chlorine) for 3 min, rinsed thoroughly and soaked in distilled water for 10 min. Seeds were germinated on Germtest paper (28 × 38 cm), moistened with Milli-Q water under sterile conditions, with a volume corresponding to twice the dry mass of the paper and kept near 100% relative humidity in the dark for 3 days. After germination, seeds were sown in 1.3 L plastic pots (one per pot) at a soil, sand, and peat ratio of 2:1:1. *V. unguiculata* cultivars were maintained under the natural conditions of semiarid region of Brazil, with daytime / nighttime temperatures of 31.0 ± 3.0 ° C / 27.0 ± 0.8 ° C, respectively, 79.8 ± 10.9% relative humidity, exposed to 12 h of natural light.

8.9 CPSMV Inoculation

Virus inoculums were prepared according to Martins et al. (2020) (MARTINS et al., 2020). Briefly, leaves of a cowpea plant genotype CE-31 (cultivar Pitiúba) infected with CPSMV (isolate CE), stored at -80 °C, were pulverized and added in a 1:10 (m / v) ratio mixture of 10 mM potassium phosphate buffer, pH 7.0, containing 0.01% (m /v) sodium bisulfite. The suspension was mixed with carborundum (mesh 500-600) (1:10, m / v) and used to inoculate plant leaves on the abaxial section, through gentle friction. Plants were inoculated at V3 stage. False-inoculated plants (mock) were treated with suspension without pulverized CPSMV-infected cowpea leaves. Treatments were performed in triplicates, with leaves collected at the times of 1 and 16 hours after application, according to Ferreira-Neto and collaborators (FERREIRA-NETO et al., 2021). Following each treatment, treated leaves were collected and immediately processed. Plants symptoms were monitored along the days after inoculation, in order to confirm CPSMV infection (Supplementary Fig. 4).

a.

b.

c.

d.

Supplementary Fig. 4 CPSMV infection symptoms in two contrastant *V. unguiculata* cultivars, 12 days after inoculation. **a** Pitiúba (susceptible) plants after false-inoculation (mock), without infection symptoms. **b** Pitiúba plants after CPSMV inoculation, showing infection symptoms, such as leaf chlorosis, leaf lamina deformation and leaf growth restriction. **c** and **d** BR 14 Mulato (resistant) plants after false-inoculation and CPSMV inoculation, respectively, both presenting absence of infection symptoms

8.10 Salicylic acid application

In order to evaluate the expression profile of the *V. unguiculata ACIN1* orthog and marker genes under salycilic acid (SA) treatment, 1mM SA in alcoholic solution was applied, according to Razmi and collaborators (2017) (RAZMI et al., 2017), with modifications. *V. unguiculata* plants from cultivar Pitiúba at V3 stage were used. As control treatment, an alcoholic solution lacking SA was applied. Treatments were performed in duplicates, with leaves collected at the times of 1 and 16 hours after application, according to Ferreira-Neto and collaborators (FERREIRA-NETO et al., 2021). After each treatment, leaves were immediately pulverized and RNA extracted using TRIzol reagent (Invitrogen), following the manufacturer's protocol.

8.11 cDNA synthesis and quantitative real-time PCR (qPCR)

The cDNA synthesis was performed using 4 ug of total RNA, oligo (dT) and Moloney murine leukemia virus reverse transcriptase (MMLV; Promega), following the manufacturer's protocol. All qPCR procedures, including testing, validation, and experiments, were conducted according to Applied Biosystems recommendations. qPCRs were performed on a QuantStudio 3 instrument (Applied Biosystems), using specific primers (Supplementary Table 2), cDNAs obtained from treatments, and GoTaq qPCR Master Mix (Promega). The amplification reactions were performed under the following conditions: 10 min at 95 °C, 45 cycles of 94 °C for 15 s and 60 °C for 1 min. *VuF-BOX3*, *VuUBQ3* and *VuL23a3* were used as reference genes for data normalization in qPCR analysis. For reference genes validation, BestKeeper software (PFAFFL et al., 2004) was used. Relative expression of *Vigna unguiculata* genes was calculated according to Pfaffl et al. (2001) (PFAFFL, 2001). Differences among means of relative expression were analyzed using ΔCq values, according to Yuan et al., (2006) (YUAN et al., 2006).

Supplementary Table 2 Primer sequences of *Vigna unguiculata* reference and target genes, gene product description, amplicon size, accession number at Phytozome database, and optimal melting temperature (Tm) of each oligonucleotide.

Gene	Gene product	Primer sequence (5′—3′)	Amplicon (bp)	Fw/ Rv Tm (°C)	Accession number
VuACIN1	Apoptotic chromatin condensation inducer in the nucleus (ACIN1)	Fw:CACACCTAAAGAGCGCATTGTT/ Rv: ATGGACGGAGGAATCGATCA	80	58/59	Vigun01g234400.1
VuPR1	Pathogenesis-related protein 1 (PR1)	Fw: CAAGGTCGCAGGTTGGTGTT/ Rv: AGTCACCTCTGCGTTGGTTTG	90	60/59	Vigun06g213100.1
VuMC1	Metacaspase-1 (MC1)	Fw: CCCACGGCCGCAAGA/ Rv: GTCGTTGATGCATCCCTTGA	80	60/58	Vigun05g144300.1
VuVSP2	Vegetative storage protein 2 (VSP2)	Fw: TGCAAACTGGGTTGCTGAAG / Rv: TGCCGAGAGACAGGAGTTTGT	80	59/59	Vigun10g178100.1
VuF-BOX3	F-box protein 3 (F-BOX3)	Fw: AAATGAATATGGCCGAAGCATT/ Rv: AATGCAGACGAGCGAACCTT	96	59/59	Vigun11g167000.1
VuUBQ3	Ubiquitin 3 (UBQ3)	Fw: TCTTGTCTTGCGACTCCGTG / Rv: TCGTGTCTGAACTCTCGACC	90	60/60	Vigun03g105700.2
*VuL23a3**	60S ribosomal protein L23a (L23a3)	Fw: CAGGGCATCATAGTCAGGT/ Rv: AGGCTTAACATCGAGTAGG	125	57.5/ 57.5	XM_014641511.1

* Retrieved from Martins et al., (2020)

REFERENCES

AKBARI-BIRGANI, Shiva *et al.* Caspases interplay with kinases and phosphatases to determine cell fate. **European Journal of Pharmacology**, [*s. l.*], v. 855, p. 20–29, 2019.

ALVES, Murilo S. *et al.* Differential expression of four soybean bZIP genes during Phakopsora pachyrhizi infection. **Functional & Integrative Genomics**, [*s. l.*], v. 15, n. 6, p. 685–696, 2015.

ARAVIND, L.; KOONIN, Eugene V. SAP – a putative DNA-binding motif involved in chromosomal organization. **Trends in Biochemical Sciences**, [*s. l.*], v. 25, n. 3, p. 112–114, 2000.

BARI, Rajendra; JONES, Jonathan D. G. Role of plant hormones in plant defence responses. **Plant Molecular Biology**, [*s. l.*], v. 69, n. 4, p. 473–488, 2009.

BARKER, David G. *et al.* Medicago truncatula, a model plant for studying the molecular genetics of theRhizobium-legume symbiosis. **Plant Molecular Biology Reporter**, [*s. l.*], v. 8, n. 1, p. 40–49, 1990.

BERGER, Susanne *et al.* Arabidopsis thaliana Atvsp is homologous to soybean VspA and VspB, genes encoding vegetative storage protein acid phosphatases, and is regulated similarly by methyl jasmonate, wounding, sugars, light and phosphate. **Plant Molecular Biology**, [*s. l.*], v. 27, n. 5, p. 933–942, 1995.

BI, Yang *et al.* Arabidopsis ACINUS is O-glycosylated and regulates transcription and alternative splicing of regulators of reproductive transitions. **Nature Communications**, [*s. l.*], v. 12, n. 1, p. 945, 2021.

BIRCH, Paul R.J. *et al.* Programmed cell death in plants in response to pathogen attack. *Em*: MOLECULAR PLANT PATHOLOGY. [*S. l.: s. n.*], 2020.

CANNON, S. B. *et al.* Legume genome evolution viewed through the Medicago truncatula and Lotus japonicus genomes. **Proceedings of the National Academy of Sciences**, [*s. l.*], v. 103, n. 40, p. 14959–14964, 2006.

CAVALCANTE, Giovanna C. *et al.* A Cell's Fate: An Overview of the Molecular Biology and Genetics of Apoptosis. **International Journal of Molecular Sciences**, [*s. l.*], v. 20, n. 17, p. 4133, 2019.

CHANG, Howard Y.; YANG, Xiaolu. Proteases for Cell Suicide: Functions and Regulation of Caspases. **Microbiology and Molecular Biology Reviews**, [*s. l.*], v. 64, n. 4, p. 821–846, 2000.

CHEN, Samuel L. *et al.* Quantitative Proteomics Reveals a Role for SERINE/ARGININE-Rich 45 in Regulating RNA Metabolism and Modulating Transcriptional Suppression via the ASAP Complex in Arabidopsis thaliana. **Frontiers in Plant Science**, [*s. l.*], v. 10, p. 1116, 2019.

CHEN, Chengjie *et al.* TBtools: An Integrative Toolkit Developed for Interactive Analyses of Big Biological Data. **Molecular Plant**, [*s. l.*], v. 13, n. 8, p. 1194–1202, 2020.

CHEN, Xiaojiang; BRUENING, George. Nucleotide sequence and genetic map of cowpea severe mosaic virus RNA 2 and comparisons with RNA 2 of other comoviruses. **Virology**, [*s. l.*], v. 187, n. 2, p. 682–692, 1992.

COLL, Nuria S. *et al. Arabidopsis* Type I Metacaspases Control Cell Death. **Science**, [*s. l.*], v. 330, n. 6009, p. 1393–1397, 2010.

DANON, Antoine *et al.* Plant programmed cell death: A common way to die. **Plant Physiology and Biochemistry**, [*s. l.*], v. 38, n. 9, p. 647–655, 2000.

DEKA, Bhagyashree; SINGH, KusumK. The arginine and serine-rich domains of Acinus modulate splicing. **Cell Biology International**, [*s. l.*], v. 43, n. 8, p. 954–959, 2019.

FERREIRA-NETO, José Ribamar Costa *et al.* The Cowpea Kinome: Genomic and Transcriptomic Analysis Under Biotic and Abiotic Stresses. **Frontiers in Plant Science**, [*s. l.*], v. 12, p. 667013, 2021.

FONG, Paulus M; TIAN, Lu; CHEN, Z Jeffrey. Arabidopsis thaliana histone deacetylase 1 (AtHD1) is localized in euchromatic regions and demonstrates histone deacetylase activity in vitro. **Cell Research**, [*s. l.*], v. 16, n. 5, p. 479–488, 2006.

FU, Zheng Qing *et al.* NPR3 and NPR4 are receptors for the immune signal salicylic acid in plants. **Nature**, [*s. l.*], v. 486, n. 7402, p. 228–232, 2012.

GALLINARI, Paola *et al.* HDACs, histone deacetylation and gene transcription: from molecular biology to cancer therapeutics. **Cell Research**, [*s. l.*], v. 17, n. 3, p. 195–211, 2007.

GOODSTEIN, David M. *et al.* Phytozome: a comparative platform for green plant genomics. **Nucleic Acids Research**, [*s. l.*], v. 40, n. D1, p. D1178–D1186, 2012.

GRANT, Murray *et al.* The RPM1 plant disease resistance gene facilitates a rapid and sustained increase in cytosolic calcium that is necessary for the oxidative burst and hypersensitive cell death. **The Plant Journal**, [*s. l.*], v. 23, n. 4, p. 441–450, 2000.

GREEN, Douglas R. The Coming Decade of Cell Death Research: Five Riddles. **Cell**, [*s. l.*], v. 177, n. 5, p. 1094–1107, 2019.

HANDBERG, Kurt; STOUGAARD, Jens. Lotus japonicus, an autogamous, diploid legume species for classical and molecular genetics. **The Plant Journal**, [*s. l.*], v. 2, n. 4, p. 487–496, 1992a.

HANDBERG, Kurt; STOUGAARD, Jens. Lotus japonicus, an autogamous, diploid legume species for classical and molecular genetics. **The Plant Journal**, [*s. l.*], v. 2, n. 4, p. 487–496, 1992b.

HAYASHI, Rippei *et al.* The exon junction complex is required for definition and excision of neighboring introns in *Drosophila*. **Genes & Development**, [*s. l.*], v. 28, n. 16, p. 1772–1785, 2014.

HU, Bo *et al.* GSDS 2.0: an upgraded gene feature visualization server. **Bioinformatics**, [*s. l.*], v. 31, n. 8, p. 1296–1297, 2015.

JOSELIN, Alvin P.; SCHULZE-OSTHOFF, Klaus; SCHWERK, Christian. Loss of Acinus Inhibits Oligonucleosomal DNA Fragmentation but Not Chromatin Condensation during Apoptosis. **Journal of Biological Chemistry**, [*s. l.*], v. 281, n. 18, p. 12475–12484, 2006.

KERR, J F R; WYLLIE, A H; CURRIE, A R. Apoptosis: A Basic Biological Phenomenon with Wideranging Implications in Tissue Kinetics. **British Journal of Cancer**, [*s. l.*], v. 26, n. 4, p. 239–257, 1972.

KIRAGA, Joanna *et al.* The relationships between the isoelectric point and: length of proteins, taxonomy and ecology of organisms. **BMC Genomics**, [*s. l.*], v. 8, n. 1, p. 163, 2007.

KUMAR, Pankaj *et al.* Genome-wide identification and expression profiling of basic leucine zipper transcription factors following abiotic stresses in potato (Solanum tuberosum L.). **PLOS ONE**, [*s. l.*], v. 16, n. 3, p. e0247864, 2021.

KUMAR, Sudhir; STECHER, Glen; TAMURA, Koichiro. MEGA7: Molecular Evolutionary Genetics Analysis Version 7.0 for Bigger Datasets. **Molecular Biology and Evolution**, [*s. l.*], v. 33, n. 7, p. 1870–1874, 2016.

LAMESCH, Philippe *et al.* The Arabidopsis Information Resource (TAIR): improved gene annotation and new tools. **Nucleic Acids Research**, [*s. l.*], v. 40, n. D1, p. D1202–D1210, 2012.

LESCOT, M. PlantCARE, a database of plant cis-acting regulatory elements and a portal to tools for in silico analysis of promoter sequences. **Nucleic Acids Research**, [*s. l.*], v. 30, n. 1, p. 325–327, 2002.

LI, Long *et al.* Genome-Wide Analysis and Expression Profiling of the Phospholipase D Gene Family in Solanum tuberosum. **Biology**, [*s. l.*], v. 10, n. 8, p. 741, 2021.

LONARDI, Stefano *et al.* The genome of cowpea (*Vigna unguiculata* [L.] Walp.). **The Plant Journal**, [*s. l.*], v. 98, n. 5, p. 767–782, 2019.

MARTINS, Thiago F. *et al.* Identification, characterization, and expression analysis of cowpea (Vigna unguiculata [L.] Walp.) miRNAs in response to cowpea severe mosaic virus (CPSMV) challenge. **Plant Cell Reports**, [*s. l.*], v. 39, n. 8, p. 1061–1078, 2020.

MICHELLE, Laetitia *et al.* Proteins Associated with the Exon Junction Complex Also Control the Alternative Splicing of Apoptotic Regulators. **Molecular and Cellular Biology**, [*s. l.*], v. 32, n. 5, p. 954–967, 2012.

MIRA, Helena; MARTÍNEZ, Noemí; PEÑARRUBIA, Lola. Expression of a vegetative-storage-protein gene from Arabidopsis is regulated by copper, senescence and ozone. **Planta**, [*s. l.*], v. 214, n. 6, p. 939–946, 2002.

MUÑOZ-AMATRIAÍN, María *et al.* Genome resources for climate-resilient cowpea, an essential crop for food security. **The Plant Journal**, [*s. l.*], v. 89, n. 5, p. 1042–1054, 2017.

MURACHELLI, Andrea Giovanni *et al.* The structure of the ASAP core complex reveals the existence of a Pinin-containing PSAP complex. **Nature Structural & Molecular Biology**, [*s. l.*], v. 19, n. 4, p. 378–386, 2012.

O'BRIEN, Mauria A.; KIRBY, Rebecca. Apoptosis: A review of pro-apoptotic and anti-apoptotic pathways and dysregulation in disease. **Journal of Veterinary Emergency and Critical Care**, [*s. l.*], v. 18, n. 6, p. 572–585, 2008.

PAIVA, Ana L. S. *et al.* Label-free Proteomic Reveals that Cowpea Severe Mosaic Virus Transiently Suppresses the Host Leaf Protein Accumulation During the Compatible Interaction with Cowpea (*Vigna unguiculata* [L.] Walp.). **Journal of Proteome Research**, [*s. l.*], v. 15, n. 12, p. 4208–4220, 2016.

PFAFFL, M. W. A new mathematical model for relative quantification in real-time RT-PCR. **Nucleic Acids Research**, [*s. l.*], v. 29, n. 9, p. 45e–445, 2001.

PFAFFL, Michael W. *et al.* Determination of stable housekeeping genes, differentially regulated target genes and sample integrity: BestKeeper – Excel-based tool using pair-wise correlations. **Biotechnology Letters**, [*s. l.*], v. 26, n. 6, p. 509–515, 2004.

PFEFFER, Claire; SINGH, Amareshwar. Apoptosis: A Target for Anticancer Therapy. **International Journal of Molecular Sciences**, [*s. l.*], v. 19, n. 2, p. 448, 2018.

QÜESTA, Julia I. *et al. Arabidopsis* transcriptional repressor VAL1 triggers Polycomb silencing at *FLC* during vernalization. **Science**, [*s. l.*], v. 353, n. 6298, p. 485–488, 2016.

RAZMI, Nasrin *et al.* Salicylic acid induced changes on antioxidant capacity, pigments and grain yield of soybean genotypes in water deficit condition. **Journal of Plant Interactions**, [*s. l.*], v. 12, n. 1, p. 457–464, 2017.

RODOR, Julie *et al.* The RNA-binding profile of Acinus, a peripheral component of the exon junction complex, reveals its role in splicing regulation. **RNA**, [*s. l.*], v. 22, n. 9, p. 1411–1426, 2016.

RYERSON, D. E.; HEATH, M. C. Cleavage of Nuclear DNA into Oligonucleosomal Fragments during Cell Death Induced by Fungal Infection or by Abiotic Treatments. **The Plant Cell**, [*s. l.*], p. 393–402, 1996.

SAHARA, Setsuko *et al.* Acinus is a caspase-3-activated protein required for apoptotic chromatin condensation. **Nature**, [*s. l.*], v. 401, n. 6749, p. 168–173, 1999.

SAKAI, Hiroaki *et al.* The *Vigna* Genome Server, '*Vig* GS': A Genomic Knowledge Base of the Genus *Vigna* Based on High-Quality, Annotated Genome Sequence of the Azuki Bean, *Vigna angularis* (Willd.) Ohwi & Ohashi. **Plant and Cell Physiology**, [*s. l.*], v. 57, n. 1, p. e2–e2, 2016.

SATO, S. *et al.* Genome Structure of the Legume, Lotus japonicus. **DNA Research**, [*s. l.*], v. 15, n. 4, p. 227–239, 2008.

SAYERS, Eric W *et al.* Database resources of the national center for biotechnology information. **Nucleic Acids Research**, [*s. l.*], v. 50, n. D1, p. D20–D26, 2022.

SCHMUTZ, Jeremy *et al.* Genome sequence of the palaeopolyploid soybean. **Nature**, [*s. l.*], v. 463, n. 7278, p. 178–183, 2010.

SCHWERK, Christian *et al.* ASAP, a Novel Protein Complex Involved in RNA Processing and Apoptosis. **Molecular and Cellular Biology**, [*s. l.*], v. 23, n. 8, p. 2981–2990, 2003.

SILVA, ERLEN KEILA CANDIDO E *et al.* AVALIAÇÃO DA RESISTÊNCIA EM POPULAÇÃO F3 ORIUNDA DO CRUZA MENTO CNC-0434 X IPA-206 DE FEIJÃO-CAUPI AO MOSAICO SEVER. [*s. l.*], 2012. p. 199–203.

SONG, Chun-Peng; GALBRAITH, David W. AtSAP18, An Orthologue of Human SAP18, is Involved in the Regulation of Salt Stress and Mediates Transcriptional Repression in Arabidopsis. **Plant Molecular Biology**, [*s. l.*], v. 60, n. 2, p. 241–257, 2006.

SOUZA, Pedro Filho Noronha; CARVALHO, Fabricio Eulálio Leite. Killing two birds with one stone: How do Plant Viruses Break Down Plant Defenses and Manipulate Cellular Processes to Replicate Themselves?. **Journal of Plant Biology**, [*s. l.*], v. 62, n. 3, p. 170–180, 2019.

TAKI, Nozomi *et al.* 12-Oxo-Phytodienoic Acid Triggers Expression of a Distinct Set of Genes and Plays a Role in Wound-Induced Gene Expression in Arabidopsis. **Plant Physiology**, [*s. l.*], v. 139, n. 3, p. 1268–1283, 2005.

VALANDRO, Fernanda *et al.* Programmed cell death (PCD) control in plants: New insights from the Arabidopsis thaliana deathosome. **Plant Science**, [*s. l.*], v. 299, p. 110603, 2020.

VAN DOORN, W. G. Classes of programmed cell death in plants, compared to those in animals. **Journal of Experimental Botany**, [*s. l.*], v. 62, n. 14, p. 4749–4761, 2011.

VUCETIC, Zivjena *et al.* Acinus-S′ Represses Retinoic Acid Receptor (RAR)-Regulated Gene Expression through Interaction with the B Domains of RARs. **Molecular and Cellular Biology**, [*s. l.*], v. 28, n. 8, p. 2549–2558, 2008.

WATANABE, Naohide; LAM, Eric. Two Arabidopsis Metacaspases AtMCP1b and AtMCP2b Are Arginine/Lysine-specific Cysteine Proteases and Activate Apoptosis-like Cell Death in Yeast. **Journal of Biological Chemistry**, [*s. l.*], v. 280, n. 15, p. 14691–14699, 2005a.

WATANABE, Naohide; LAM, Eric. Two Arabidopsis Metacaspases AtMCP1b and AtMCP2b Are Arginine/Lysine-specific Cysteine Proteases and Activate Apoptosis-like Cell Death in Yeast. **Journal of Biological Chemistry**, [*s. l.*], v. 280, n. 15, p. 14691–14699, 2005b.

XU, Qixian; ZHANG, Lingrui. Plant caspase-like proteases in plant programmed cell death. **Plant Signaling & Behavior**, [*s. l.*], v. 4, n. 9, p. 902–904, 2009.

YUAN, Joshua S *et al.* Statistical analysis of real-time PCR data. **BMC Bioinformatics**, [*s. l.*], v. 7, n. 1, p. 85, 2006.

ZERMATI, Yael *et al.* Caspase Activation Is Required for Terminal Erythroid Differentiation. **Journal of Experimental Medicine**, [*s. l.*], v. 193, n. 2, p. 247–254, 2001.

ZHANG, Jiaoping *et al.* Genome-wide association study for flowering time, maturity dates and plant height in early maturing soybean (Glycine max) germplasm. **BMC Genomics**, [*s. l.*], v. 16, n. 1, p. 217, 2015.